AMERICAN SOCIETY FOR MICROBIOLOGY | Journal of Virology®

VIRUS-CELL INTERACTIONS

GRP78 Is an Important Host Factor for Japanese Encephalitis Virus Entry and Replication in Mammalian Cells

Minu Nain,[a,b] Sriparna Mukherjee,[c] Sonali Porey Karmakar,[a] Adrienne W. Paton,[d] James C. Paton,[d] M. Z. Abdin,[b] Anirban Basu,[c] Manjula Kalia,[a] Sudhanshu Vrati[a,e]

Vaccine and Infectious Disease Research Centre, Translational Health Science and Technology Institute, NCR Biotech Science Cluster, Faridabad, India[a]; Department of Biotechnology, Faculty of Science, Jamia Hamdard, New Delhi, India[b]; National Brain Research Centre, Manesar, Haryana, India[c]; Research Centre for Infectious Diseases, Department of Molecular and Cellular Biology, University of Adelaide, Adelaide, Australia[d]; Regional Centre for Biotechnology, NCR Biotech Science Cluster, Faridabad, India[e]

ABSTRACT Japanese encephalitis virus (JEV), a mosquito-borne flavivirus, is the leading cause of viral encephalitis in Southeast Asia with potential to become a global pathogen. Here, we identify glucose-regulated protein 78 (GRP78) as an important host protein for virus entry and replication. Using the plasma membrane fractions from mouse neuronal (Neuro2a) cells, mass spectroscopy analysis identified GRP78 as a protein interacting with recombinant JEV envelope protein domain III. GRP78 was found to be expressed on the plasma membranes of Neuro2a cells, mouse primary neurons, and human epithelial Huh-7 cells. Antibodies against GRP78 significantly inhibited JEV entry in all three cell types, suggesting an important role of the protein in virus entry. Depletion of GRP78 by small interfering RNA (siRNA) significantly blocked JEV entry into Neuro2a cells, further supporting its role in virus uptake. Immunofluorescence studies showed extensive colocalization of GRP78 with JEV envelope protein in virus-infected cells. This interaction was also confirmed by immunoprecipitation studies. Additionally, GRP78 was shown to have an important role in JEV replication, as treatment of cells post-virus entry with subtilase cytotoxin that specifically cleaved GRP78 led to a substantial reduction in viral RNA replication and protein synthesis, resulting in significantly reduced extracellular virus titers. Our results indicate that GRP78, an endoplasmic reticulum chaperon of the HSP70 family, is a novel host factor involved at multiple steps of the JEV life cycle and could be a potential therapeutic target.

IMPORTANCE Recent years have seen a rapid spread of mosquito-borne diseases caused by flaviviruses. The flavivirus family includes West Nile, dengue, Japanese encephalitis, and Zika viruses, which are major threats to public health with potential to become global pathogens. JEV is the major cause of viral encephalitis in several parts of Southeast Asia, affecting a predominantly pediatric population with a high mortality rate. This study is focused on identification of crucial host factors that could be targeted to cripple virus infection and ultimately lead to development of effective antivirals. We have identified a cellular protein, GRP78, that plays a dual role in virus entry and virus replication, two crucial steps of the virus life cycle, and thus is a novel host factor that could be a potential therapeutic target.

KEYWORDS Japanese encephalitis virus, flavivirus, host-cell interactions, receptors, viral replication, virus entry

Received 22 November 2016 **Accepted** 27 December 2016

Accepted manuscript posted online 4 January 2017

Citation Nain M, Mukherjee S, Karmakar SP, Paton AW, Paton JC, Abdin MZ, Basu A, Kalia M, Vrati S. 2017. GRP78 is an important host factor for Japanese encephalitis virus entry and replication in mammalian cells. J Virol 91:e02274-16. https://doi.org/10.1128/JVI.02274-16.

Editor Michael S. Diamond, Washington University School of Medicine

Address correspondence to Manjula Kalia, manjula@thsti.res.in, or Sudhanshu Vrati, vrati@thsti.res.in.

Japanese encephalitis virus (JEV), belonging to the family *Flaviviridae*, is a neurotropic virus causing encephalitis in humans, with a mortality rate of up to 30% (1–3). The family also contains other mosquito-borne, medically important pathogens, such as

dengue virus (DENV), West Nile virus (WNV), and tick-borne encephalitis virus (TBEV). Host factors crucial for virus entry and replication can be potential targets for the development of novel therapeutics.

The JEV virion has a glycoprotein envelope that encloses a capsid containing the positive-sense viral RNA genome of ~11 kb. The viral RNA has 5′ and 3′ untranslated regions flanking a single open reading frame that encodes a 3,432-amino-acid (aa) polyprotein. The polyprotein is cleaved into three structural proteins, capsid (C), precursor membrane (prM), and envelope (E), and seven nonstructural proteins, NS1, NS2A, NS2B, NS3, NS4A, NS4B, and NS5 (4).

The virus envelope, which is the determinant of virus entry into the cell, comprises a heterodimer of membrane (M) and E proteins. The E protein has a highly variable oligomeric state that undergoes pH-induced conformational changes during virus entry. The protein consists of an N-terminal ectodomain, a stem region, and a transmembrane domain. The ectodomain has three structurally distinct domains, I, II, and III. The crystal structure of the JEV E protein has been described at a resolution of 2.1 Å (5). The immunoglobulin-like E protein domain III (ED3) projects from the mature virion surface and has been shown to play a major role in receptor binding in the cases of DENV and TBEV (6–9).

Studies have shown that heparan sulfate proteoglycans (HSPGs) and glycosaminoglycans (GAGs) serve as attachment factors for JEV (10–12). These interactions are charge driven, with the negatively charged HSPGs serving to concentrate the positively charged E glycoprotein-containing virions on the cell membrane, thus facilitating the receptor interaction. The heparan sulfate (HS)-binding protein lactoferrin inhibits JEV infection by inhibiting JEV-HS interaction (10). DC-SIGN has also been shown to act as an attachment factor for JEV on human dendritic cells (13). Several other studies have attempted to identify the JEV receptor, with virus overlay protein-binding assay (VOPBA) being a popular technique. This involves virus binding to membrane proteins resolved on SDS-PAGE based on the assumption that the virus particle would specifically bind to its receptor protein. Though this technique has limitations, it has been widely employed in several studies, most likely because of its technical ease. Thus, proteins that have been suggested to play a role in JEV entry are HSP70, vimentin, laminin receptor, CD4, $\alpha 5\beta 3$ integrin, and DC-SIGN (14–18).

In the present study, we have characterized JEV ED3 as the receptor-binding domain of E protein and have identified glucose-regulated protein 78 (GRP78) as a membrane protein that interacts with JEV E protein in mammalian cells. GRP78 is a ubiquitously expressed endoplasmic reticulum (ER) chaperone that helps in proper folding of proteins into their secondary structure (19). It is also a critical regulator of ER stress, maintains calcium homeostasis in the ER, acts as an antiapoptotic protein, and plays important roles in angiogenesis and tumor progression (20, 21). Besides the ER, GRP78 is also localized to the cell surfaces of several cell types (22–27). Though some studies suggest that GRP78-interacting proteins may be involved in its transport to the plasma membrane, the exact mechanism is not clear (26, 28–30).

Here, we demonstrate that GRP78 expressed on the surfaces of neuronal and epithelial cells is important for JEV entry into the cell. Furthermore, GRP78 was shown to be crucial for virus replication, as specific cleavage of GRP78 with subtilase toxin (SubAB) subsequent to virus uptake prevented viral RNA replication and translation of viral proteins, resulting in a significant block in production of infectious JEV virions. Together, these data show an important role of GRP78 in JEV uptake into mammalian cells and in virus replication postentry, two crucial steps in the JEV life cycle.

RESULTS

JEV ED3 as an exploratory molecule to identify JEV receptor. Antibody mapping on WNV and DENV have demonstrated that several neutralizing epitopes are located on ED3 (31). The crystal structure of JEV E protein demonstrated that key residues that bind to neutralizing antibodies are located on the domain III lateral ridge, in addition to the domain I-II hinge and the domain I lateral ridge (5). Thus, JEV ED3 could harbor a

potential site for virus interaction with its cellular receptor. We therefore tested JEV ED3 as an exploratory molecule for identification of the virus receptor. JEV ED3 and JEV NS3 proteins were produced as His-tagged proteins in *Escherichia coli*. The identities of the two proteins were confirmed by Western blotting with JEV E, NS3, and His tag antibodies (Fig. 1A). Fluorophore (Alexa 568)-coupled ED3 was found to bind the membranes of Neuro2a cells by immunofluorescence microscopy (Fig. 1B). Under the same conditions, Alexa 568-coupled NS3 protein (used as a negative control) showed no binding to Neuro2a cells.

Studies have shown that the ED3 domain of the virus envelope can inhibit entry of DENV, WNV, and JEV (32–35). To test if the ED3 generated in our study could compete with JEV binding to cells (as measured by productive infection, leading to JEV RNA replication, and the virus yield), Neuro2a cells were incubated with JEV ED3 or JEV NS3 for 1 h on ice, followed by infection with JEV. While NS3 did not inhibit JEV infection, ED3 showed a significant reduction in JEV replication (~86 to 96%) and virus yield (~96%) at different multiplicities of infection (MOI) in a dose-dependent manner (Fig. 1C). These data showing ED3 competition with JEV for Neuro2a infection validated the potential of ED3 for study of the JEV receptor.

Identification of GRP78 as a JEV ED3-interacting membrane protein. To identify the membrane protein(s) interacting with JEV ED3, Neuro2a cell membrane proteins were biotinylated, and a cell fraction enriched in the plasma membrane proteins was isolated. This was used to immunoprecipitate JEV ED3-interacting proteins, which were separated on a 2-dimensional (2D) gel and silver stained. Compared to the control (immunoprecipitation without ED3), four unique protein spots were recognized and were subjected to mass spectrometry (MS) (Fig. 2A). The "score" of the proteins identified is the sum of the scores of the individual peptides, and a higher score indicates higher confidence in the identification. One of the proteins was identified as GRP78, and this was further confirmed by Western blotting with a GRP78-specific antibody. The interaction between JEV ED3 and GRP78 was further validated by coimmunoprecipitation studies in Neuro2a cells (Fig. 2B).

We also employed the mammalian 2-hybrid system to check for interaction between JEV ED3 and GRP78 (Fig. 2C). The cDNA for JEV ED3 was cloned in the pACT vector (containing the DNA binding domain), while GRP78 cDNA was cloned in the pBIND vector (containing the transcriptional activation domain). Interaction between the two proteins results in transcription of the firefly luciferase gene. The pBIND vector also expresses *Renilla* luciferase, which helps to normalize transfection efficiency. The positive-control plasmids and JEV ED3-pACT and GRP78-pBIND were transfected into HEK 293T cells with the corresponding empty pBIND or pACT vector or together. Transfection of JEV ED3-pACT and GRP78-pBIND together showed very high relative luciferase activity, thus confirming the interaction between JEV-ED3 and GRP78 (Fig. 2C).

GRP78 is known to be an ER-resident chaperone protein but has also been reported to be present on the plasma membranes of several cell types, including neurons (22–27, 30). For GRP78 to be involved in JEV entry, it must be located on the cell membrane. To examine this, we analyzed the staining patterns of GRP78 on both permeabilized and nonpermeabilized cells (Fig. 3A). Three cell types—primary mouse neurons and Neuro2a and Huh-7 cells—were fixed, permeabilized, and stained with either secondary antibody alone (as a negative control) (Fig. 3A, left) or GRP78 primary and Alexa 488-coupled anti-rabbit secondary antibodies (Fig. 3A, middle). For exclusive plasma membrane staining, cells were incubated with GRP78 antibody on ice for 1 h, followed by fixation of the cells (Fig. 3A, right). While permeabilized cells showed extensive intracellular GRP78 staining, the nonpermeabilized cells clearly showed surface localization of the protein (Fig. 3A, center versus right). Surface localization of GRP78 was further validated by Western blotting of plasma membrane fractions from Neuro2a and Huh-7 cells (Fig. 3B). The purity of the plasma membrane fractionation was confirmed

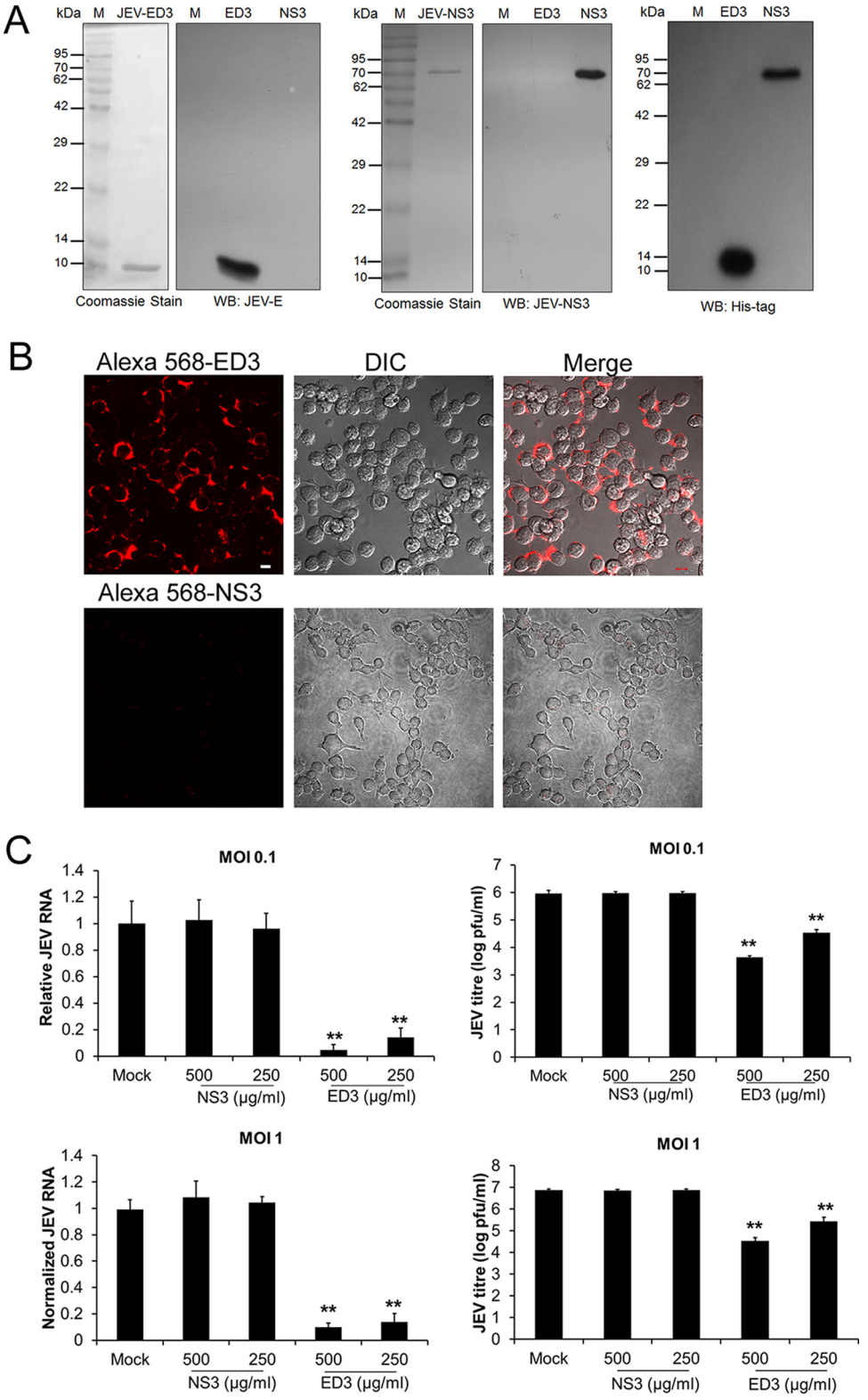

FIG 1 JEV ED3 binds to Neuro2a cells and inhibits JEV infection. (A) His-tagged recombinant JEV ED3 and JEV NS3 were expressed in *E. coli* and purified on an Ni-NTA column. The purified proteins were electrophoresed on an SDS-PAGE gel, followed by Coomassie staining or Western blotting with JEV E, JEV NS3, and His tag antibodies. (B) Alexa 568-coupled JEV ED3 was added to Neuro2a cells on ice for 1 h. The cells were washed, fixed, and imaged on a confocal microscope. Cells were similarly treated with Alexa 568-labeled JEV NS3 protein as a negative control. (Left) JEV ED3 or NS3 binding on cells. (Middle) DIC image of the field. (Right) Merge of the two images. Bar, 10 μm. (C) Neuro2a cells were incubated with JEV ED3 or NS3 proteins at the indicated concentrations on ice for 1 h, followed by infection with JEV at an MOI of 0.1 or 1. At 24 h p.i., JEV RNA levels were determined by qRT-PCR (left),

(Continued on next page)

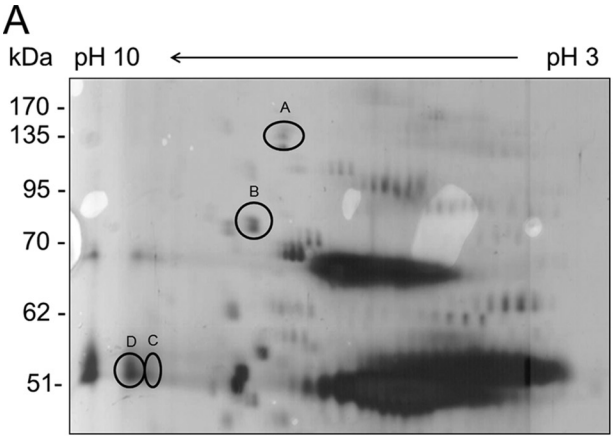

Spot	MW (kDa)	Score	Molecule identified
A	~200	101.37	Filaggrin-2 OS=Homo sapiens GN=FLG2 PE=1 SV=1 - [FILA2_HUMAN]
B	~78	181.43	78 kDa glucose-regulated protein OS=Mus musculus GN=Hspa5 PE=1 SV=3 - [GRP78_MOUSE]
C	~50	60.21	Ig gamma-1 chain C region, membrane-bound form OS=Mus musculus GN=Ighg1 PE=1 SV=2 - [IGH1M_MOUSE]
D	~50	51.31	Ig gamma-1 chain C region secreted form OS=Mus musculus GN=Ighg1 PE=1 SV=1 - [IGHG1_MOUSE]

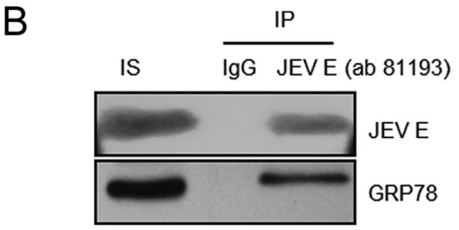

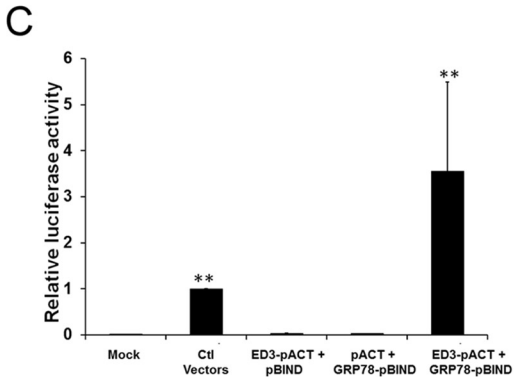

FIG 2 JEV ED3 interacts with GRP78. (A) JEV-ED3-interacting proteins from plasma membrane fractions of Neuro2a cells were separated on a 2D gel and silver stained. Four unique spots (circled) were excised and subjected to mass spectroscopy analysis. The table on the right shows mass spectrometry scores and identities for the unique spots seen on the 2D gel. (B) Neuro2a cell lysate was incubated with JEV ED3, followed by immunoprecipitation (IP) with either mouse IgG or mouse JEV E antibody (ab81193). The input sample (IS) and the immunoprecipitated samples were electrophoresed and Western blotted with JEV E and GRP78 antibodies. (C) The cDNAs for JEV ED3 and mouse GRP78 were cloned in pACT and pBIND vectors, respectively, of the mammalian two-hybrid system. HEK 293T cells were mock transfected or transfected with positive-control (Ctl) vectors: ED3-pACT plus pBIND, pACT plus GRP78-pBIND, and ED3-pACT plus GRP78-pBIND. The cells were lysed 24 h posttransfection, and luciferase activity was determined. The luciferase activity in cells transfected with positive-control plasmids was taken as 1 for normalization. The luciferase activity in transfected cells was compared to that in mock-transfected cells; **, $P < 0.01$. Each experiment was performed with biological duplicates, and the data presented are from three independent experiments. The error bars indicate SD.

by Western blotting with glyceraldehyde-3-phosphate dehydrogenase (GAPDH) (a cytosolic marker) and calreticulin (an ER marker) antibodies (Fig. 3B).

Role of GRP78 in JEV binding to the cell membrane and virus entry. GRP78 contains four hydrophobic domains that may form transmembrane helices with both the N and C termini localized outside the membrane (36). The N terminus has regulatory domains governing binding and signaling, while the C terminus is the ATPase domain (28). In the above-described experiments, we demonstrated the binding of JEV ED3 to GRP78 on the cell membrane and its interference with JEV infection of the cell. To further examine the role of GRP78 in virus entry, we performed virus binding experiments on Neuro2a cells in the presence of GRP78 antibodies. Purified JEV was labeled with the lipophilic dye DiI (Vybrant DiI cell labeling solution; Thermo Fisher Scientific) as described previously (37). Labeled virus particles retain infectivity and can be used to detect single-particle JEV entry events (37). Based on the fluorescence

FIG 1 Legend (Continued)
and the infectious-virus titer (right) in the culture soup was determined by plaque assay. (Left) Relative JEV RNA for each condition normalized to mock treatment. (Right) Absolute values of JEV titers. Viral RNA level or titers in protein-treated cells were compared with those in the mock-treated cells. **, $P < 0.01$. Each experiment was done with biological duplicates, and similar trends were observed in four independent experiments. The error bars indicate SD.

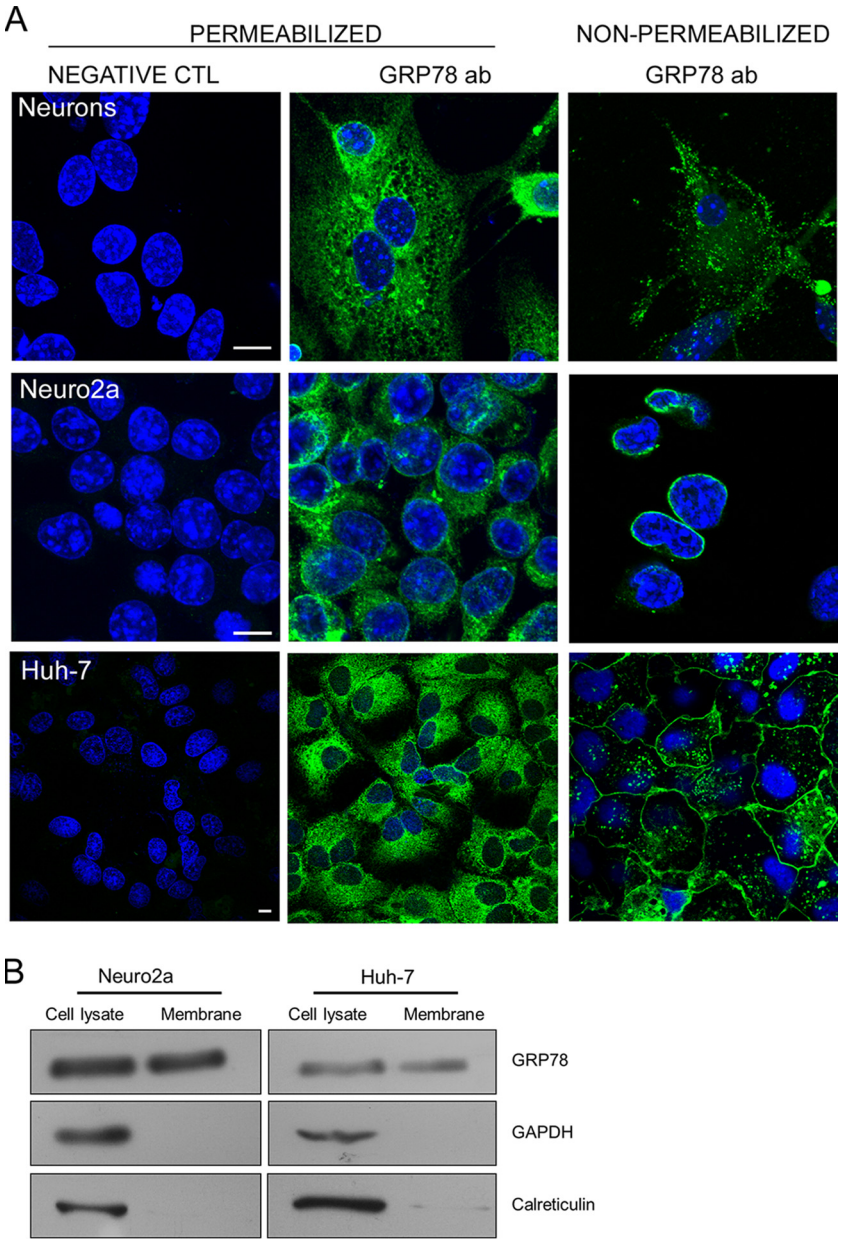

FIG 3 GRP78 localizes on the plasma membrane in mammalian cells. (A) (Middle) Primary mouse cortical neurons and Neuro2a and Huh-7 cells were fixed, permeabilized, and stained with GRP78 and Alexa 488 anti-rabbit antibodies. (Left) As a negative control for specificity of antibody staining, cells were incubated with Alexa 488 anti-rabbit antibody alone. (Right) Cells were incubated with rabbit GRP78 antibody on ice for 1 h, followed by incubation with Alexa 488 anti-rabbit antibody. The cells were fixed and imaged on a confocal microscope. The nuclei were stained with DAPI (blue). Bars, 10 μm. (B) Total cell lysates and the purified plasma membrane fractions of Neuro2a and Huh-7 cells were Western blotted with GRP78 antibody. Western blotting with GAPDH and calreticulin antibodies was done to rule out contamination with ER membranes and to validate the protein fractionation.

intensity of labeled virus particles, a quantitative estimation of JEV binding on cells can be done. Neuro2a cells were preincubated with antibodies against the N- or C-terminal domain of GRP78 or rabbit IgG (negative control) on ice for 1 h, followed by washes with chilled phosphate-buffered saline (PBS) and addition of DiI-labeled JEV at an MOI of 50 for 1 h, after which the cells were washed, fixed, and imaged. The images clearly showed markedly reduced fluorescence on cells treated with GRP78 N-terminal antibody (Fig. 4A). Quantitative analysis confirmed that cells treated with the N-terminal GRP78 antibody had significantly reduced (~38%) virus

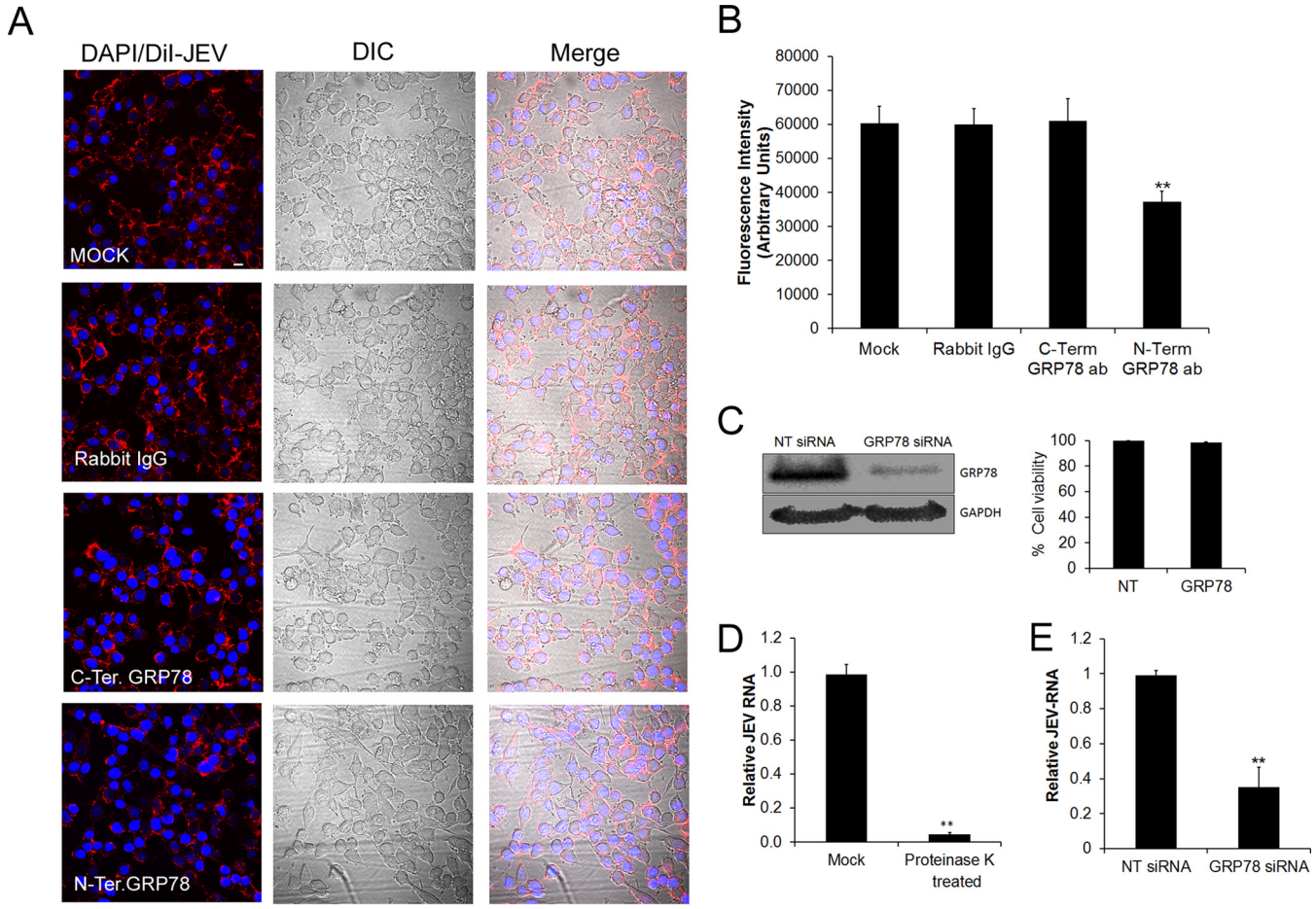

FIG 4 Role of GRP78 in binding and entry of JEV in neuronal cells. (A) Neuro2a cells were mock treated or incubated with 100 μg/ml rabbit IgG or GRP78 C- and N-terminus-specific antibodies on ice for 1 h, followed by the addition of DiI-labeled JEV (MOI, 50) for 1 h. The cells were washed, fixed, and imaged on a confocal microscope. Red fluorescence on the cell membrane indicates virus binding. (B) Quantitation of DiI-labeled JEV binding on cells was done as described in Materials and Methods. Shown are the means of integrated intensities of DiI signals for the different treatments. The intensities recorded under different treatments were compared to that seen on the mock-treated cells (**, $P < 0.01$). Similar results were seen in two independent experiments. Error bars indicate standard error of the mean (SEM). (C) (Left) Neuro2a cells were transfected with NT or GRP78 siRNAs that caused a significant reduction in GRP78 protein levels in cells 48 h later. (Right) The viability of cells at 48 h of siRNA treatment was tested by MTT assay. The treatment did not affect cell viability. (D) Neuro2a cells were incubated on ice with JEV at an MOI of 5 for 1 h. Mock or proteinase K treatment was followed by incubation at 37°C for 2 h, after which relative endocytosed JEV RNA levels were determined by qRT-PCR. The RNA levels in proteinase K-treated cells were compared to that in the mock-treated cells (taken as 1). The proteinase K treatment efficiently removed membrane-bound virus, resulting in a very significant reduction (**, $P < 0.01$) in the levels of endocytosed viral RNA. The experiment was performed in biological duplicates, and similar results were seen in three independent experiments. (E) NT control siRNA- or GRP78 siRNA-treated Neuro2a cells were infected with JEV (MOI, 5) 48 h after transfection. This was followed by proteinase K treatment, as described in Materials and Methods, to remove any unbound virus. The endocytosed-virus levels at 2 h p.i. were determined by qRT-PCR for JEV genomic RNA. The level of JEV RNA in NT siRNA-treated cells was taken as 1 for determining the relative RNA levels in GRP78 siRNA-treated cells. The level of endocytosed viral RNA in GRP78 siRNA-treated cells was compared to that seen in mock-treated cells (**, $P < 0.01$). The experiment was performed in biological duplicates, and the results presented are from three independent experiments. The error bars indicate SD.

binding, whereas the C-terminal GRP78 antibody and the nonspecific rabbit IgG failed to affect virus binding (Fig. 4B).

To further examine the role of GRP78 in JEV binding and entry into cells, the protein was depleted by small interfering RNAs (siRNAs) in Neuro2a cells. The siRNA treatment caused a significant decrease in GRP78 mRNA (data not shown) and ~80% decrease at the protein level, while it did not affect cell viability (Fig. 4C). At this stage, cells were infected with JEV at an MOI of 5 for 1 h, followed by proteinase K treatment. This treatment ensures that any bound but noninternalized virion particles are removed from the host membrane (Fig. 4D). Virus entry into GRP78-depleted cells was measured by quantification of JEV RNA in cells at 2 h postinfection (p.i.). JEV RNA at this early time point would be a direct measure of JEV entry, since viral RNA replication in the cell can be detected only at 4 to 5 h p.i. (our unpublished observations). Compared to cells

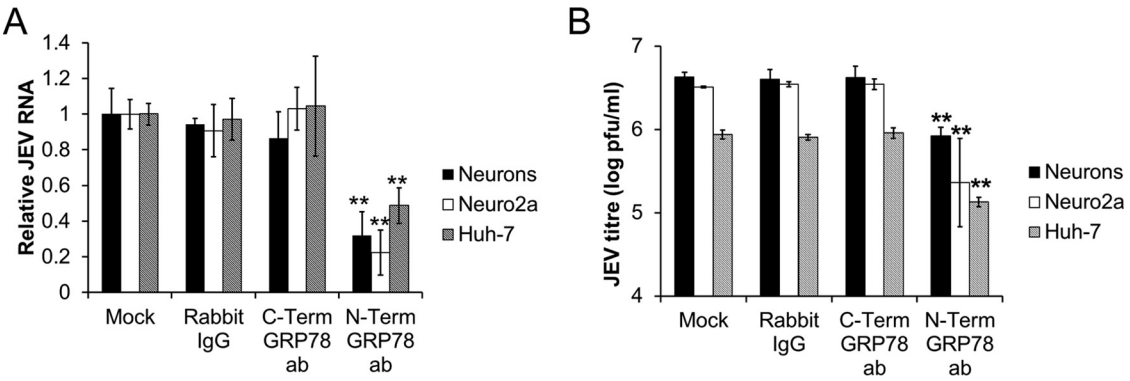

FIG 5 GRP78 N-terminal antibody inhibits JEV infection in mammalian cells. Primary mouse cortical neurons and Neuro2a and Huh-7 cells were mock treated or incubated with 100 μg/ml rabbit IgG or GRP78 C- and N-terminus-specific rabbit antibodies on ice for 1 h, followed by JEV infection at an MOI of 1. Viral RNA levels (A) and titers (B) were determined at 24 h p.i. The level of JEV RNA in mock-treated cells was taken as 1 for determining the relative RNA levels. The viral RNA levels and titers were compared to those in mock-treated cells (**, $P < 0.01$). Each experiment contained biological duplicates, and the data presented are from three independent experiments. The error bars indicate SD.

treated with nontargeting (NT) siRNA, the GRP78 siRNA-treated cells showed a significant (~60%) reduction in JEV RNA levels (Fig. 4E), indicating a role of GRP78 in JEV uptake and entry into Neuro2a cells.

We further validated the role of GRP78 in JEV entry in multiple cell types. Primary mouse cortical neurons and Neuro2a and Huh-7 cells were mock treated or preincubated with antibodies against the N- or C-terminal domain of GRP78 or rabbit IgG (negative control), followed by JEV infection. While the C-terminal antibodies had no effect, the N-terminal GRP78 antibodies showed significant ~68%, 75%, and 50% decreases ($P < 0.01$) in JEV RNA levels 24 h p.i. in mouse cortical neurons and Neuro2a and Huh-7 cells, respectively (Fig. 5A). The N-terminal antibody also caused significant 80%, 90%, and 84% reductions ($P < 0.01$) of JEV titers in mouse cortical neurons and Neuro2a and Huh-7 cells, respectively, while the titers with the C-terminal antibody were not significantly different from those seen in mock- and rabbit IgG-treated cells (Fig. 5B).

Collectively, the significantly reduced virus binding to cells in the presence of GRP78 antibody, substantially reduced virus uptake into GRP78 siRNA-treated cells, and significant (almost 1-log-unit) reduction in the extracellular viral titers in the presence of GRP78 antibody establish a role for GRP78 in JEV binding and entry into the mammalian cells.

GRP78 localization on the cell membrane occurs via interactions with other proteins, and its translocation mechanism is cell type dependent (38). The protein has been shown to be a part of the receptor complex, along with major histocompatibility class I (MHC-I) for coxsackievirus A9 entry (27). We tested if antibodies against MHC-I could block JEV infection of Neuro2a cells. Pretreatment of cells with MHC-I antibodies significantly inhibited JEV infection (~80% reduction; $P < 0.01$); however, no further enhancement of this inhibition was observed by the addition of GRP78 antibody (Fig. 6). It is thus likely that GRP78 associates with MHC-I on the plasma membrane in neuronal cells.

GRP78 interacts with the JEV E protein in virus-infected cells. GRP78 is an ER chaperone and has been shown to regulate viral antigen production for DENV (39). We further tested if ER-resident GRP78 shows colocalization with JEV E protein in virus-infected cells. JEV-infected Neuro2a and Huh-7 cells (Fig. 7A) were permeabilized and stained with GRP78 and JEV E antibodies. Extensive overlap was observed between GRP78 and JEV E proteins in both Neuro2a and Huh-7 cells, with colocalization indexes of 0.85 and 0.77, respectively. This interaction was further validated by pulldown experiments. JEV E protein from total lysate of virus-infected cells was immunoprecipitated using JEV E antibody and tested for coimmunoprecipitation of GRP78. Indeed,

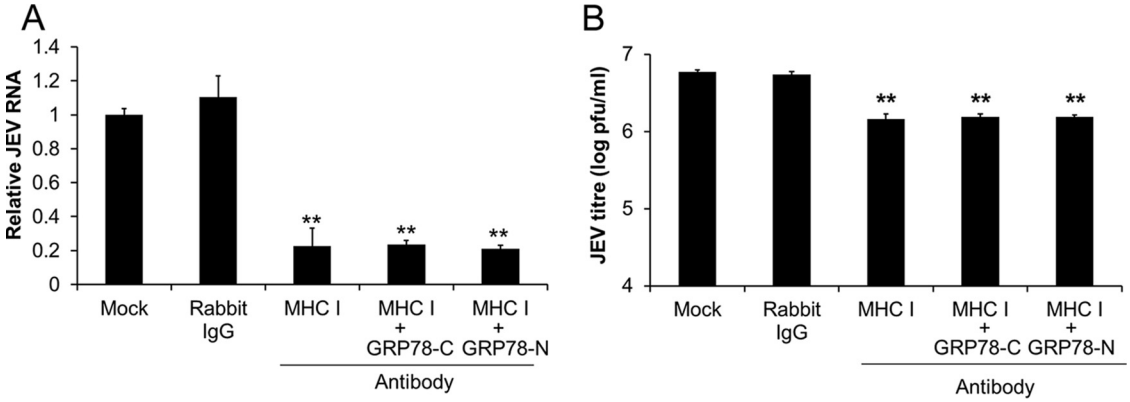

FIG 6 Antibodies against MHC I inhibit JEV infection. Neuro2a cells were mock treated or incubated with 100 μg/ml rabbit IgG or MHC-I antibody alone or in combination with GRP78 C- and N-terminus-specific rabbit antibodies on ice for 1 h, followed by JEV infection at an MOI of 1. Viral RNA levels (A) and titers (B) were determined at 24 h p.i. The level of JEV RNA in mock-treated cells was taken as 1 for determining the relative RNA levels. The JEV RNA levels and viral titers were compared to those in mock-treated cells (**, $P < 0.01$). Each experiment contained biological duplicates, and the data presented are from three independent experiments. The error bars indicate SD.

GRP78 was seen to associate with JEV E protein in virus-infected cells (Fig. 7B). We further tested this with a reverse pulldown in which GRP78 was immunoprecipitated and was seen to associate with the JEV E protein in Neuro2a cells (Fig. 7C).

Role of GRP78 in JEV replication. To further examine the role of GRP78 in JEV infection, cells were treated with SubAB toxin. This is an AB5 toxin derived from Shiga toxigenic *E. coli* strains that can specifically cleave GRP78 into 44-kDa and 28-kDa fragments, corresponding to the N- and C-terminal regions of GRP78, respectively, leading to its inactivation (40). The $SubA_{A272}B$ mutant lacks the catalytic ability of SubAB to cleave GRP78 (40). Primary mouse cortical neurons and Neuro2a and Huh-7 cells were mock treated or treated with 50 or 100 ng/ml SubAB or $SubA_{A272}B$ toxin. At these concentrations, 24-h treatment with the toxin did not affect cell viability as tested by MTT [3-(4,5-dimethyl-2-thiazolyl)-2,5-diphenyl-2H-tetrazolium bromide] assay (Fig. 8A). The effect of the toxin on JEV infectivity was checked by treating virions with 50 or 100 ng/ml SubAB or $SubA_{A272}B$ toxin for 1 h, followed by plaque assays (Fig. 8B). The SubAB toxin effectively cleaved GRP78 in both Neuro2a and Huh-7 cells, as seen by a decrease in the intensity of the 78-kDa full-length GRP78 band and appearance of the C-terminal fragment of 28 kDa that can be detected with the C-terminus-specific antibody on Western blotting (Fig. 8C). As expected, the $SubA_{A272}B$ toxin had no effect on GRP78.

To test the effect of GRP78 cleavage on JEV replication, virus-infected cells were treated with SubAB or $SubA_{A272}B$ toxin at 1, 6, and 12 h p.i., and the presence of the toxin was maintained until 24 h p.i. SubAB toxin treatment at 1 h p.i. effectively blocked virus replication, with up to 99% reduction in viral RNA levels in all cell types (Fig. 9A, left). The effect of the toxin on neuronal cells (both primary neurons and Neuro2a cells) was most pronounced, with ~85% decrease in viral RNA levels when added at 6 or 12 h p.i., while in Huh-7 cells, 30 to 75% inhibition was observed (Fig. 9B and C, left). The reduction in JEV RNA levels also resulted in significantly reduced viral titers (Fig. 9A, B, and C, right). Thus, JEV titers decreased by 98, 82, and 59% in Huh-7 cells when the toxin was added at 1, 6, and 12 h p.i., respectively, at a concentration of 50 ng/ml. Neuronal cells showed a higher degree of sensitivity to SubAB toxin treatment than Huh-7 cells, with 95 to 99% reduction in viral titers. Notably, no virus was detectable when cells were treated 1 h p.i. with SubAB toxin at 100 ng/ml. These data collectively suggest that GRP78 has an important role in JEV replication and production of extracellular virions.

To further confirm the role of GRP78 in JEV replication and to rule out the potential effects of virus spread and entry in a second round of infection, we performed the

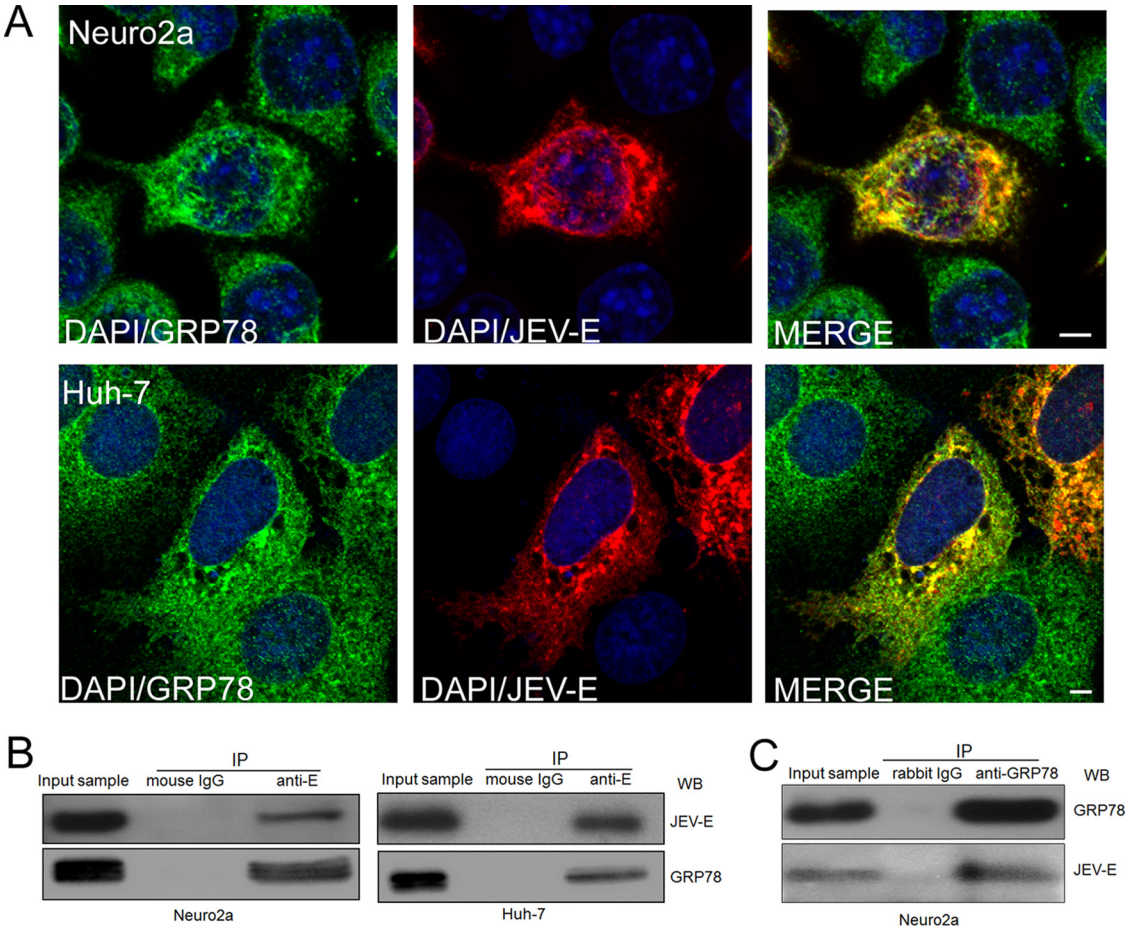

FIG 7 GRP78 colocalizes and interacts with JEV E protein in virus-infected cells. (A) Neuro2a and Huh-7 cells were infected with JEV at an MOI of 5. The cells were fixed 24 h p.i., permeabilized, and stained with GRP78 and JEV E primary antibodies, followed by Alexa 488 anti-rabbit and Alexa 568 anti-mouse antibodies. Cells were imaged on a confocal microscope using a 60×, NA 1.42 objective. Bars, 5 μm. Extensive colocalization of JEV E and GRP78 proteins can be clearly seen in the JEV-infected cells. (B) Neuro2a and Huh-7 cells were infected with JEV at an MOI of 5, and cell lysates were prepared 24 h p.i. They were used for immunoprecipitation with mouse IgG or JEV ED3 (ab81193) antibody. The cell lysates (input samples) and the immunoprecipitates were Western blotted with JEV E (ab26950) and GRP78 antibodies. (C) Lysate from JEV-infected (MOI, 5; 24 h p.i.) Neuro2a cells was immunoprecipitated using rabbit IgG or GRP78 antibody, followed by Western blotting with GRP78 and JEV E (ab81193) antibodies.

above-described experiment at a very high MOI of 50. This ensured that nearly all cells (~99%) were infected in the first round of infection, as seen by the expression of the JEV envelope protein at 6 h p.i. (Fig. 10A). The virus-infected cells were treated with SubAB or $SubA_{A272}B$ toxin at 1 h p.i., and the toxin was maintained in the culture medium until 6 h p.i., after which the JEV RNA levels were assayed (Fig. 10B). The 6-h p.i. time point was chosen because no virions have been released in the culture supernatant by this early time of the infection cycle, and thus, a second round of infection has not initiated. SubAB toxin treatment effectively blocked virus replication, with up to 90% reduction in viral RNA levels in all cell types, demonstrating an important role of GRP78 in JEV replication postentry (Fig. 10B).

Studies on the kinetics of JEV entry into Neuro2a cells have demonstrated that virus uncoating and fusion with the endosome occur by 1 h p.i. (37). Virus replication is detectable in cells by 6 to 8 h p.i., as seen from double-stranded RNA (dsRNA) foci (41). These dsRNA puncta show extensive colocalization with JEV NS1, NS3, and NS5 nonstructural proteins (41, 42). To test if GRP78 had any role in the formation of the replication complex, we performed immunofluorescence staining of dsRNA and NS3 in JEV-infected Neuro2a cells treated with wild-type or mutant toxin at 6 h p.i. (Fig. 11). Indeed, at 24 h p.i., while mock-treated and mutant-toxin-treated cells showed replication complexes marked by colocalization of dsRNA and NS3, the cells treated with

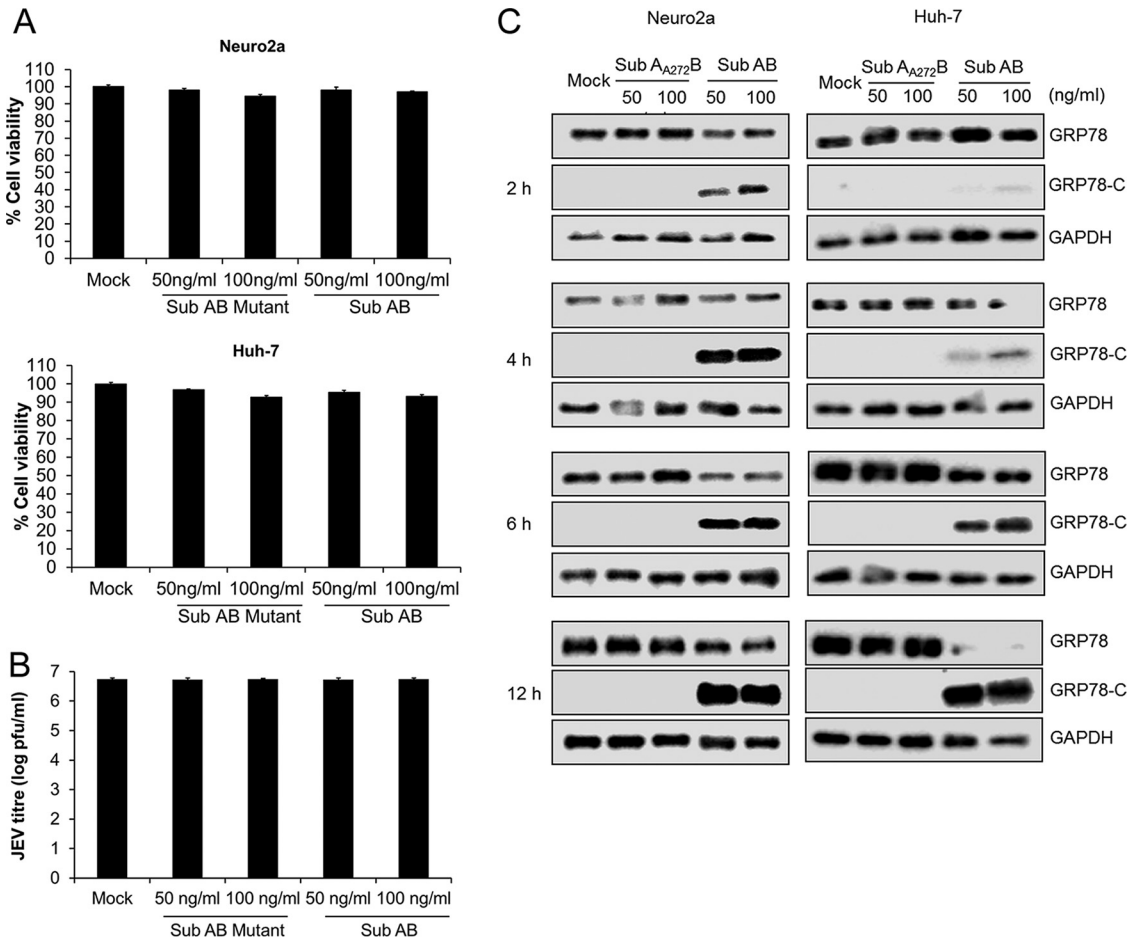

FIG 8 Toxicity of subtilase cytotoxin and its biological activity. (A) Neuro2a and Huh-7 cells were treated with $SubA_{A272}B$ or SubAB toxin at the indicated concentrations for 24 h, followed by MTT assay. Shown is cell viability under different treatments, which was not affected by toxin treatment. (B) Purified JEV virions were mock incubated or incubated with $SubA_{A272}B$ or SubAB toxin at the indicated concentrations for 1 h, followed by plaque assays to determine virus viability and infectivity. JEV viability and infectivity were not affected by the toxin treatment. The data shown are representative of the results of three independent experiments, each with biological duplicates. (C) Neuro2a and Huh-7 cells were incubated with $SubA_{272}B$ or SubAB toxin for 2, 4, 6, and 12 h. Cell lysates were run on an SDS-PAGE gel and Western blotted with GRP78, GRP78-C (C-terminal), and GAPDH (loading control) antibodies. GRP78 cleavage is shown by a decrease in the intensity of the 72-kDa band of the full-length GRP78 and appearance of the C-terminal fragment of 28 kDa that can be detected with the C-terminus-specific antibody. The error bars indicate SD.

SubAB toxin showed an almost complete absence of replication complexes. This manifested in a nearly complete block in production of viral proteins (Fig. 11B). Thus, JEV NS1, E, and NS3 proteins were not seen in cells treated with SubAB toxin, whereas their levels were not affected in mutant-toxin-treated cells compared to that in the mock-treated cells. This is consistent with the absence of the extracellular virus production in the presence of the SubAB toxin seen in the previous experiment.

We further tested the role of GRP78 in virus replication by transfecting the JEV RNA into the GRP78-depleted Neuro2a cells, thus bypassing the JEV entry step (Fig. 12). The JEV RNA used in the study was infectious, as seen by viral RNA replication, translation of viral proteins, and production of infectious virions. Transfection of 300 ng of JEV RNA resulted in nearly ~75% of cells being infected, as seen from the expression of JEV envelope protein at 6 h posttransfection (Fig. 12A). Transfection of viral RNA in GRP78-depleted cells (treated with GRP78 siRNAs) resulted in significantly decreased levels of JEV RNA (~60%), viral proteins (~60%), and extracellular viral titers (~75%) (Fig. 12B to D) compared to those in the NT siRNA-treated control cells. Collectively, these data indicate that GRP78 is an important host factor for JEV replication at a postentry step.

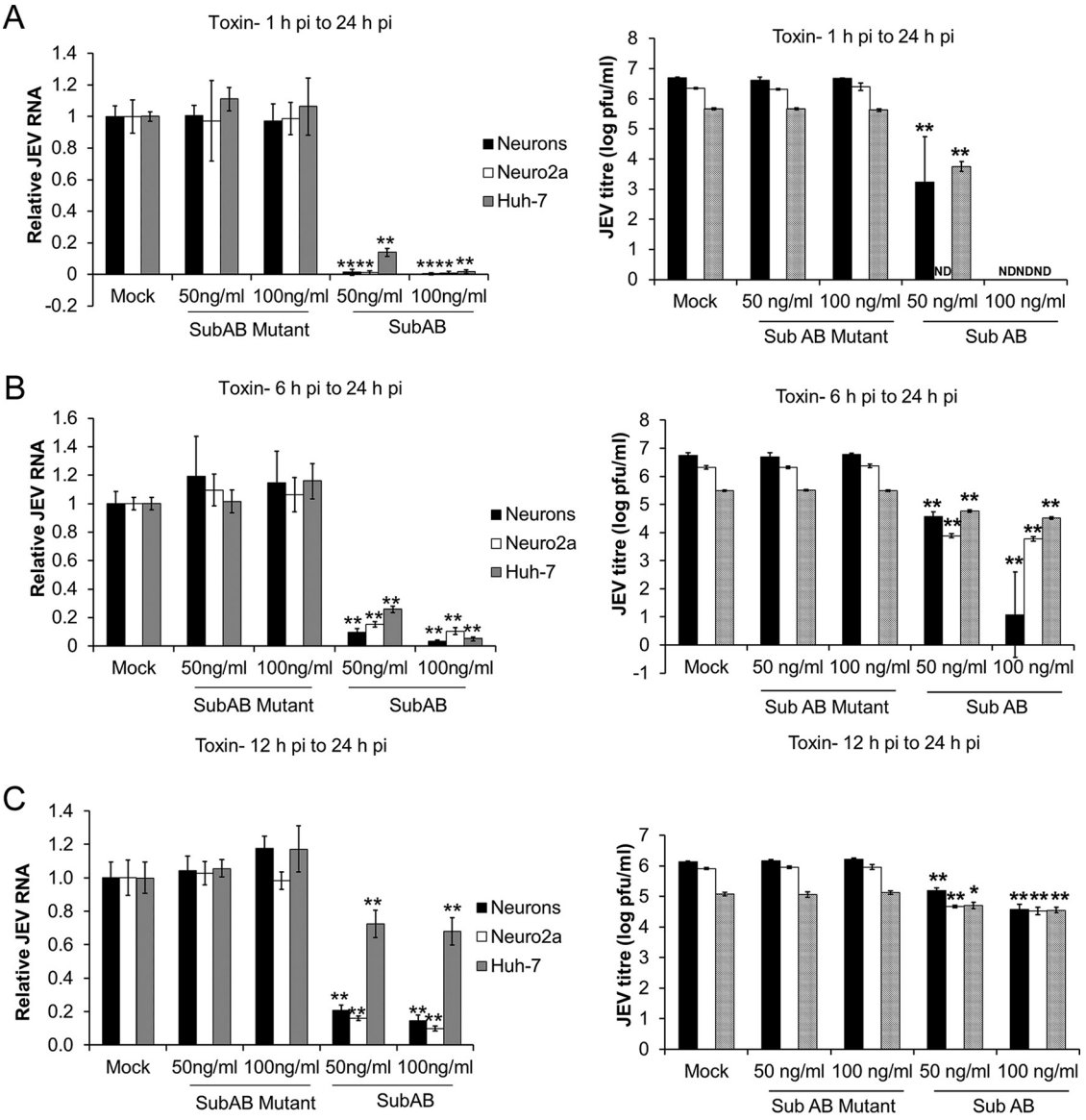

FIG 9 Role of GRP78 in JEV replication. Primary mouse cortical neurons and Neuro2a and Huh-7 cells were infected with JEV at an MOI of 1, followed by mock treatment or addition of SubAB or $SubA_{A272}B$ toxin at 1 (A), 6 (B), or 12 (C) h p.i. (Left) JEV RNA levels were determined 24 h p.i. by qRT-PCR. The JEV RNA level in mock-treated cells was taken as 1 for determining the relative RNA levels. (Right) Virus titers were determined by plaque assays at 24 h p.i. The JEV RNA levels and viral titers were compared with that in mock-treated cells (*, $P < 0.05$; **, $P < 0.01$; ND, not determined). Each experiment contained biological duplicates, and the data presented are from three independent experiments. The error bars indicate SD.

DISCUSSION

GRP78, also known as the immunoglobulin heavy chain binding protein or BiP, was first described as an ER chaperone involved in folding and translocation of peptides (19). Recent studies have highlighted multiple functions of the protein, and it has been implicated in cancer and inflammatory and autoimmune diseases (21, 43, 44). Here, we show that GRP78 is involved in multiple steps of the JEV life cycle ranging from receptor binding and entry to replication, highlighting its important role in virus infection.

Using JEV ED3 as an exploratory molecule to fish out putative receptor proteins from plasma membrane fractions of neuronal cells, our study identified GRP78 as an ED3-interacting protein. Biochemical binding studies indicated that GRP78 and JEV ED3 and E proteins showed strong interaction. Further, by antibody inhibition and siRNA-mediated depletion of GRP78, we demonstrated an important role for the protein in JEV entry in multiple cell types.

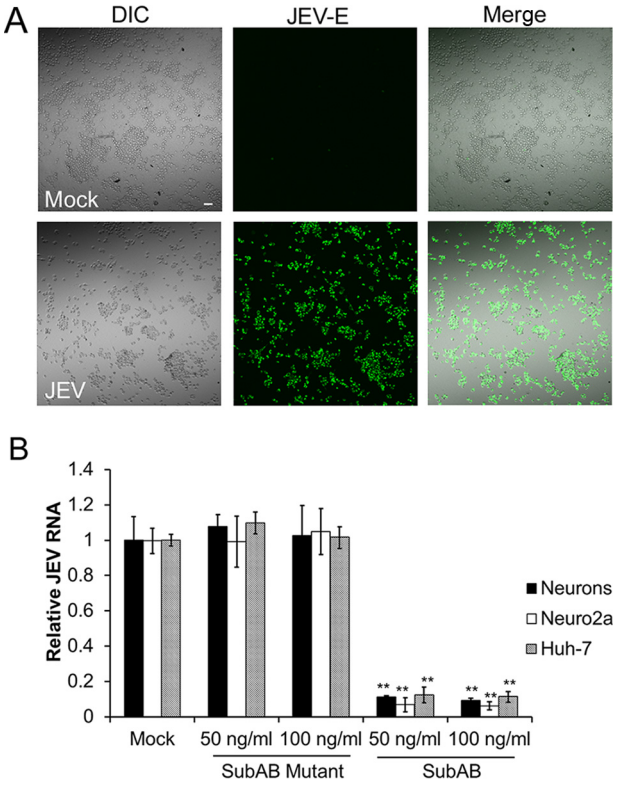

FIG 10 Role of GRP78 in JEV replication. (A) Neuro2a cells were either mock infected (top) or infected with JEV at an MOI of 50 (bottom). At 6 h p.i., the cells were fixed and stained with JEV E antibody and imaged. (Left) DIC images. (Middle) JEV-E staining. (Right) Merge of the two. Bar, 10 μm. (B) Primary mouse cortical neurons and Neuro2a and Huh-7 cells were infected with JEV at an MOI of 50, followed by mock treatment or addition of SubAB or $SubA_{A272}B$ toxin at 1 h p.i. JEV RNA levels were determined at 6 h p.i. by qRT-PCR. The JEV RNA levels were compared with that in the mock-treated cells (**, $P < 0.01$). Each experiment contained biological duplicates, and the data presented are from three independent experiments. The error bars indicate SD.

GRP78 levels on the plasma membrane are generally considered to be low under normal physiological conditions, with increased levels seen in cancer cells and under conditions of cellular stress. However, several studies have shown that GRP78 is copiously localized under normal conditions on the plasma membrane in different cell types, including endothelial cells, monocytes, and neurons, carrying out varied functions (22–27, 30). GRP78 on the plasma membrane functions as a cell surface signaling receptor for activated α2-macroglobulin (45). The protein has been shown to be associated with the MHC-I molecule on the surfaces of human umbilical vein endothelial cells (HUVEC) and green monkey kidney cells (27, 30) and with T-cadherin on the surfaces of HUVEC, where it functions as a signaling receptor (26). Localization of GRP78 on the plasma membrane has also been shown for mouse hippocampal neurons (22, 24). In our study, we observed that GRP78 was localized on the plasma membrane in primary mouse cortical neurons and neuronal and epithelial cells, enabling it to participate in the virus entry process.

GRP78 was also shown to be a cellular receptor for DENV-2 on HepG2 cells by VOPBA and mass spectrometry studies, and interestingly, antibodies against the N terminus of GRP78 inhibited DENV-2 infection of HepG2 cells (25). GRP78 interacts with Borna disease virus (BDV) glycoprotein 1 (GP1) at the cell surface, and anti-GRP78 antibodies reduced GP1 binding and BDV infection of permissive human oligodendroglial OL cells and HEK 293T cells (24). Specific interaction between GRP78 and BDV GP1 in infected cells was also confirmed by immunoprecipitation analysis.

Our studies indicate that GRP78 is involved in JEV binding and entry into mammalian cells, highlighting its important role in the early stages of virus infection. The

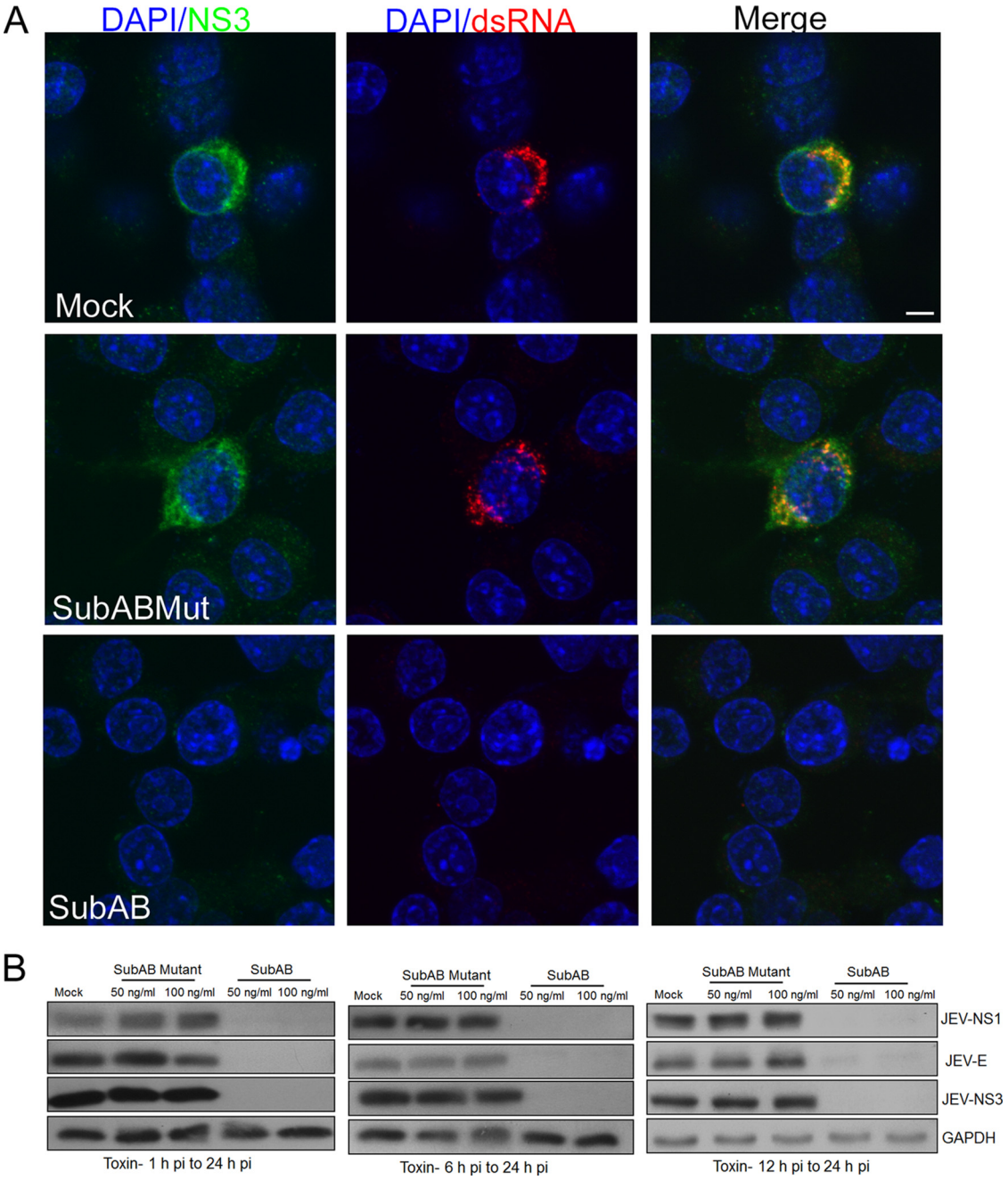

FIG 11 SubAB toxin prevents the formation of JEV replication complexes. (A) Neuro2a cells were infected with JEV at an MOI of 1, and 6 h p.i., were mock treated (top) or treated with $SubA_{A272}B$ mutant (middle) or SubAB (bottom) toxin. The cells were fixed at 24 h p.i. and stained with dsRNA (red) and JEV NS3 (green) antibodies. Cells were imaged on a confocal microscope. Bar, 5 μm. (B) The lysates from cells treated as for panel A (JEV at an MOI of 5) were Western blotted to study the levels of JEV E, NS1, and NS3 proteins. GAPDH was used as a loading control.

immunoglobulin heavy chain binding function of GRP78 may be important in this interaction, as the ED3 domain of flaviviruses has an immunoglobulin-like structure (7, 8). JEV is a neurotropic virus that actively infects both neuronal and nonneuronal cells. The ubiquitous presence of GRP78 on different cell types may thus allow JEV to use the protein to infect the various cell types. While data presented here clearly show an important role for GRP78 in JEV binding and uptake, experiments in a GRP78-deficient cell type would help establish its role as a JEV receptor. However, a GRP78-deficient cell line could not be found or produced, indicating the essential nature of the protein.

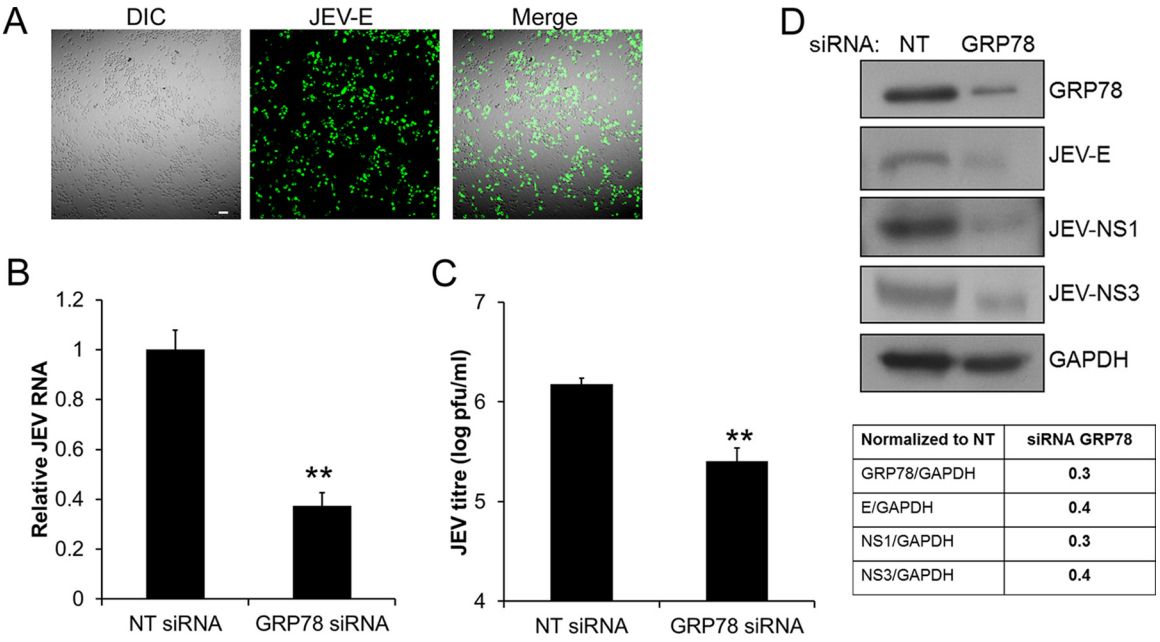

Normalized to NT	siRNA GRP78
GRP78/GAPDH	**0.3**
E/GAPDH	**0.4**
NS1/GAPDH	**0.3**
NS3/GAPDH	**0.4**

FIG 12 GRP78 is an important host factor for JEV replication postentry. (A) Neuro2a cells were transfected with 300 ng JEV RNA, and at 6 h posttransfection, the cells were fixed and stained with JEV E antibody. (Left) DIC image. (Middle) JEV E staining. (Right) Merge of the two. Bar, 10 μm. (B to D) Neuro2a cells were transfected with NT or GRP78 siRNAs and 48 h later were transfected with 300 ng purified JEV RNA. At 24 h post-JEV RNA transfection, cells were processed for estimation of relative JEV RNA levels (B) and Western blotted for the indicated antibodies (D), and virus titers in the culture supernatant were determined by plaque assays (C). Each experiment contained biological duplicates, and the data presented in panels B and C are from three independent experiments. (D) The ratios of band intensities for different JEV antibodies and GAPDH are shown below the Western blots. The levels of viral RNA and titers in GRP78 siRNA-treated cells were compared to that in the NT siRNA-treated cells (**, $P < 0.01$). The error bars indicate SD.

GRP78 functions as part of the receptor complex, along with MHC-I, for coxsackievirus A9 entry (27). Antibodies against MHC-I blocked JEV infection of Neuro2a cells, but no enhancement of the inhibition was observed by the addition of N-terminal GRP78 antibody. It is possible that GRP78 on the plasma membrane is closely associated with MHC-I in neuronal cells, as has been reported previously for endothelial cells (27, 30). In such a scenario, antibody to either of the two proteins could sterically hinder the binding of JEV to its receptor, resulting in the inhibition of virus infection of the host cell. Alternately, while GRP78 is involved in JEV binding, MHC-I may be involved in virus internalization, similar to what has been reported for coxsackievirus A9 (27). A recent study has shown that GRP78 anchors on the cell membrane via interactions with other proteins and that its translocation mechanism is cell context dependent (38). GRP78 has been reported to interact with diverse proteins, such as voltage-dependent anion channel (46) and the DnaJ-like protein MTJ-1 (28). All of these proteins are known to associate with lipid rafts in the plasma membrane (47–49). Interestingly, lipid rafts and some of the proteins associated with them are implicated in JEV infection of mammalian cells (50). The potential roles of MHC-I and other lipid raft proteins associated with GRP78 in JEV infection need to be examined further.

Considering the broad host range of JEV and the fact that the GRP78 antibodies did not completely abolish virus infection, it is highly likely that additional molecules besides GRP78 act as JEV receptors. Indeed, other molecules, such as HSP70, $\alpha5\beta3$ integrin, and DC-SIGN, have been reported to be involved in JEV entry into various cell types (13–16). Additional studies on primary cells and animal models are essential to better understand the JEV receptor system.

In addition to the well-characterized role of GRP78 as a chaperone assisting the folding of several proteins, it has also been shown to bind to several viral glycoproteins, where it is involved in the correct folding and maturation of the envelope (29, 51–58). Since the JEV E protein also shows extensive colocalization with GRP78 in infected cells and this association was further confirmed by immunoprecipitation studies, it is highly

likely that GRP78 is also involved in the correct folding of the JEV E protein and virus packaging. It is also possible that GRP78 is involved in folding of a protein(s) required for JEV replication.

Subtilase cytotoxin, by its specificity for GRP78, has proven to be a powerful tool to elucidate its function (40). Cleavage of GRP78 with SubAB led to significant inhibition of human cytomegalovirus formation but had little effect on viral protein synthesis (59). Similarly, cleavage of GRP78 with SubAB resulted in a significant reduction of DENV antigen accumulation and a 10- to 100-fold decrease in infectious-virus release; however, RNA levels were unchanged (39). In our study, SubAB treatment at different times post-virus infection resulted in a significant block in JEV replication. This block was nearly complete when the toxin was added at 1 h p.i. and very significant at both 6 h p.i. and 12 h p.i. Previous studies in our laboratory have shown that virus replication complexes are established in the infected cell by 6 to 8 h p.i. (41, 42). They are detectable as discrete foci of dsRNA and viral nonstructural proteins, like NS1, NS3, and NS5, by immunofluorescence (42). Inhibition of virus replication by the addition of SubAB toxin at 6 and 12 h p.i. strongly implies a crucial role of GRP78 post-viral entry in viral RNA translation and replication. Transfection of JEV RNA in GRP78-depleted cells showed inhibition of RNA replication, viral protein synthesis, and extracellular virus production, strongly supporting our observation that GRP78 has an important role in JEV replication.

RNA interference studies have demonstrated an essential role of GRP78 in maturation and egress of rotavirus and DENV (60, 61). GRP78 was also identified as a protein that was secreted from JEV-infected BHK-21 cells and was associated with JEV virions (62). The same study also showed that knockdown of GRP78 impaired mature-virus production but had no effect on NS1 production. However, we did not observe GRP78 to be associated with virus preparations used in our study.

Virus replication is a complex process controlled by several host proteins and pathways. Our study highlights the important role of GRP78 at several critical nodes of the virus life cycle, ranging from entry to replication. While GRP78 cleavage inhibits dengue virus antigen production and assembly of virions (39), its effect on viral genome replication has not been reported for any virus. GRP78 is complexed with ER stress sensors and regulates the unfolded-protein response (UPR) (63, 64). Induction of UPR and GRP78 upregulation has been shown for several viruses, including JEV (65–67). Subtilase cytotoxin cleavage of GRP78 also activates the ER stress pathways (68, 69) and facilitates ER-associated degradation (ERAD) (70). Since ER stress pathways and ERAD are closely associated with JEV replication (42, 67, 71), it is also possible that the effect of GRP78 cleavage on JEV replication is manifested by dysregulation of these cellular pathways. The multiple critical roles of GRP78 in the infectious life cycle of JEV highlight the potential of this host protein as a novel target for antiviral development against JEV.

MATERIALS AND METHODS

Ethics statement. Animal experiments for the generation of primary mouse cortical neurons were conducted at the National Brain Research Centre and were approved by the institutional ethics committee (protocol no. NBRC/IAEC/2014/96). Animals were monitored with good care according to the guidelines of the Committee for the Purpose of Control and Supervision of Experiments on Animals (CPCSEA), Government of India.

Cells and virus. Mouse neuroblastoma (Neuro2a), human hepatocellular carcinoma (Huh-7), human embryonic kidney (HEK293T), and porcine stable kidney (PS) cells were obtained from the Cell Repository at the National Centre for Cell Sciences, Pune, India. Neuro2a, Huh-7, and HEK 293T cells were grown in Dulbecco's modified Eagle's medium (DMEM) (Invitrogen) supplemented with 10% fetal bovine serum (FBS) (HyClone). PS cells were grown in Eagle's minimal essential medium (MEM) with 10% FBS. All media were additionally supplemented with 100 μg/ml penicillin-streptomycin and 2 mM L-glutamine. The P20778 isolate of JEV grown in PS cells was used in the studies described here. JEV was concentrated by polyethylene glycol precipitation and purified over a 20% sucrose cushion at 80,000 $\times$ *g* for 4 h at 4°C. The purified virus was exchanged into PBS through an additional ultracentrifugation step. The purity of the preparation for the absence of GRP78 was established by Western blotting.

Reagents and antibodies. Antibodies against JEV E protein (ab41671, mouse; ab81193, mouse; ab26950, rabbit), GRP78 N terminus (ab32618, rabbit), GRP78 C terminus (ab21685, rabbit), MHC-I (ab52922, rabbit), and calreticulin (ab22683, mouse) were purchased from Abcam, while antibody against GAPDH (2118S, mouse) was purchased from Cell Signaling Technology. The dsRNA antibody (J2, mouse)

was purchased from English and Scientific Consulting Bt. Antibody against His tag (P5A11, mouse) was obtained from the Developmental Studies Hybridoma Bank. Fluorescent secondary antibodies and ProLong Gold anti-fade reagent with DAPI (4′,6-diamidino-2-phenylindole) (P36935) were obtained from Invitrogen. Horseradish peroxidase (HRP)-coupled secondary antibodies were obtained from Jackson Immunochemicals. Rabbit polyclonal antibodies against JEV NS1 and NS3 were produced in the laboratory and have been described previously (42). All the JEV antibodies used in the study reacted with proteins of the expected sizes on Western blotting in JEV-infected cells, but not in mock-infected cells. The staining specificity of the rabbit polyclonal antisera and commercial antibodies was confirmed by immunofluorescence in mock- and JEV-infected cells. Optimum working dilutions and lack of cross-reactivity with cellular proteins was established for all the primary and secondary antibodies.

Mouse cortical neuron culture. Primary cortical neuron culture was done following the previously published protocol (72) with minor modifications. Briefly, postnatal-day-0 to postnatal-day-2 BALB/c mouse pups were decapitated aseptically, and cortices were collected in calcium-magnesium-free Tyrode solution, pH 7.4 (0.8% NaCl, 0.03% KCl, 0.2% glucose, 0.05% NaH_2PO_4, 0.025% KH_2PO_4, 0.008% $NaHCO_3$). Tissue samples were chopped and digested with trypsin and DNase to make single-cell suspensions. Cells were passed through 127-μm-pore-size nylon mesh (Sefar) to remove debris and then centrifuged to collect the final cell pellet. The cells from the resuspended pellet were counted in a hemocytometer and seeded in either a poly-D-lysine (Sigma)-coated 96-well plate or a 24-well plate according to need. Initial cell culture was done in neurobasal medium supplemented with L-glutamine (2 mM), 1% glucose, 5% FBS, 10% horse serum, and penicillin-streptomycin. After 48 h, when the cells had adhered, serum was removed from the medium to reduce glial growth. For experimental treatment purposes, neurobasal medium was replaced with DMEM containing N2, B27 supplements, and antibiotics. To ensure complete glial absence, cells were treated with arabinoside (10 μM) 1 day before experiments.

Cloning, expression, and purification of JEV ED3 and NS3 proteins. The cDNA encoding ED3 (aa 303 to 398) of JEV E protein and JEV NS3 (aa 1505 to 2123; GenBank accession number AF080251) was cloned with a C-terminal His tag in the pET28a vector (Novagen). The identities of the clones were confirmed by nucleotide sequencing. Proteins were expressed in *E. coli* BL-21(DE3) cells (Invitrogen). Briefly, transformed bacteria were grown at 37°C until an optical density at 600 nm (OD_{600}) of 0.6 to 0.8 was reached, and protein expression was induced by adding 100 mM IPTG (isopropyl-β-D-thiogalactopyranoside). The induced bacterial pellet was dissolved under denaturing conditions in 8 M urea buffer (100 mM NaH_2PO_4, 10 mM Tris-HCl, 8 M urea, pH 8.0). For protein purification, Ni-nitrilotiracetic acid (NTA) beads (Qiagen) were added to the lysate. The protein was eluted in 8 M urea, pH 4.5, and dialyzed sequentially against 4 M urea, 1 M urea, and PBS. JEV ED3 was seen as a single band of ~10 kDa, and NS3 was seen as an ~70-kDa band on an SDS-PAGE gel. The protein concentration was determined with a Bradford protein assay kit (Bio-Rad).

Isolation of JEV ED3-interacting membrane proteins. JEV ED3 protein was immobilized on protein A beads (Pierce) using an anti-JEV E protein antibody (ab81193). Plasma membrane proteins from Neuro2a cells were extracted using a cell surface protein isolation kit (Pierce). Isolated membrane proteins were added to JEV ED3-immobilized beads, and the pulled-down proteins (JEV ED3-interacting proteins) were analyzed further by 2D gel electrophoresis (GE Healthcare) and silver staining (Pierce). The ED3 protein was omitted in the negative control. Briefly, the rehydration buffer (7 M urea, 2 M thiourea, 2% CHAPS {3-[(3-cholamidopropyl)-dimethylammonio]-1-propanesulfonate}, 2% pharmalyte [GE Healthcare], 0.002% bromophenol blue) was added to the beads after immunoprecipitation. The sample was loaded on a pH 3 to 10 strip (GE Healthcare). After resolution of the samples based on their pIs, the samples were electrophoresed on an SDS-PAGE gel to resolve proteins on the basis of their individual sizes. The SDS-PAGE gel was then silver stained, and the protein spots unique to the sample (not seen in the negative control) were analyzed by MS performed at the Centre for Cellular and Molecular Platforms (C-CAMP), Bengaluru, India. Briefly, identification and sequencing of protein in the band of interest was done using in-gel and in-solution tryptic digestion. Tryptic-digested peptides were subjected to a standard nano-reverse phase liquid chromatography (nano-RP-LC) (70-min gradient) run, followed by LTQ-Orbitrap tandem-MS (MS-MS) analysis. The results were analyzed on MASCOT using proteome discoverer 1.3 with Swiss-Prot as the database. High-confidence peptides with a prerequisite of a minimum of two peptides leading to identification of proteins were selected, and a list was generated. The label-free peak-area-based quantification value of identified proteins was provided. The protein "score" displays the standard score—the cumulative protein score based on summing the ion scores of the unique peptides. A higher score indicates a higher confidence of identification.

Mammalian two-hybrid studies. The CheckMate mammalian two-hybrid system (Promega) was used to study JEV ED3 interaction with GRP78. Firefly luciferase in the reporter vector is transcribed in response to interaction between two proteins cloned in a pACT vector and a pBIND vector. The cDNA for JEV ED3 was cloned in a pACT vector and that for mouse GRP78 in a pBIND vector. ED3-pACT, GRP78-pBIND, and a reporter vector were cotransfected into HEK293T cells in a 1:1:1 ratio using Lipofectamine 2000 (Invitrogen). At 24 h posttransfection, the cells were lysed in 1× passive lysis buffer, and the luciferase activity was determined using a dual-luciferase assay kit (Promega) on an Orion II microplate luminometer (Berthold). *Renilla* luciferase denotes transfection efficiency, as it is present in the pBIND vector, whereas firefly luciferase measures interaction between ED3 and GRP78. The activity of firefly luciferase was normalized to that of *Renilla* luciferase.

qRT-PCR for JEV RNA. Cells were given the appropriate treatment/infection, and RNA was extracted following lysis in TRIzol reagent. The cDNA was prepared using random hexamers. To determine JEV RNA copies in infected cells, quantitative real-time (qRT) PCR was done using TaqMan probes, and GAPDH was used as an internal control. JEV RNA was amplified using the following probes: TaqMan probe, CCACG

CCACTCGACCCATAGACTG (5′-end 6-carboxyfluorescein [FAM], 3′-end 6-carboxytetramethylrhodamine [TAMRA]); 5′ primer, AGAGCACCAAGGGAATGAAATAGT; 3′ primer, AATAAGTTGTAGTTGGGCACTCTG. GAPDH was used as an internal control: TaqMan probe, ACAACCTGGTCCTCAGTGTAGC (5′-end FAM, 3′-end TAMRA); 5′ primer, CCTGCCAAGTATGATGAC; 3′ primer, GGAGTTGCTGTTGAAGTC. The mouse GRP78 primers used were as follows: 5′ primer, ACTTGGGGACCACCTATTCCT; 3′-primer, ATCGCCAATCA GACGCTCC. The PCR conditions were as follows: 94°C for 2 min (1 cycle) and 94°C for 15 s, 55°C for 30 s, and 72°C for 1 min (40 cycles). The qRT-PCR was done on an Applied Biosystems ABI 7500 instrument. Each experiment contained biological duplicates, and qPCR for each sample was done in technical triplicates. The fold change in the expression level of JEV RNA levels is represented as the mean and standard deviation (SD) of the results of three independent experiments.

Protein inhibition assays for JEV infection. To examine if JEV ED3 could competitively inhibit JEV infection, Neuro2a cells were incubated with purified JEV ED3 or NS3 at a concentration of 250 to 500 μg/ml at 4°C for 1 h, followed by JEV infection at an MOI of 0.1 to 1. After 24 h, the cells were lysed in TRIzol reagent, and JEV RNA levels were determined by qRT-PCR. Virus titers in the supernatant of infected cells were estimated by plaque assays (73).

Virus-labeling and antibody inhibition assays for JEV binding. Purified virus was labeled with DiI by injecting 2 nmol dye into virus stock under vortexing for 10 min at room temperature. Excess dye was removed by purification through Micro Spin G-25 columns (GE Healthcare). This protocol results in a homogeneously labeled particle suspension, as seen by confocal microscopy of labeled particles attached to glass coverslips. The DiI signal is specific for JEV and was confirmed independently by immunostaining with JEV envelope antibody (37). Labeled virus was used immediately for experiments and tested in parallel for infectivity by plaque assays.

To check for the effect of GRP78 antibodies on JEV binding, Neuro2a cells were incubated with 100 μg/ml of the specific GRP78 rabbit antibodies or rabbit IgG (negative control) for 1 h on ice. After two washes with chilled PBS, DiI-labeled JEV (MOI, ~50) was added to the cells for 1 h on ice, followed by washes with chilled PBS, fixation, and imaging on a confocal microscope. For quantification of JEV binding on cells, the cell outline was marked using the differential interference contrast (DIC) image, and the integrated fluorescence intensity (DiI fluorescence) per cell was calculated. Each experiment was done with biological duplicates for each condition, and 10 to 12 fields were imaged per sample (35 to 50 cells/sample). The results were presented as the mean ± standard error of the mean (SEM) of the integrated intensity from biological duplicates of one representative experiment. Similar results were obtained from two independent experiments.

siRNA depletion and virus entry. NT and mouse GRP78-targeting siRNAs were purchased from Dharmacon (On-Target plus Smart Pool). Mammalian cells were transfected with siRNAs according to the manufacturer's recommendations and harvested 24 and 48 h later to check for protein knockdown. GRP78 mRNA levels were checked by qRT-PCR, and the protein knockdown in Neuro2a cells was determined by Western blotting with GRP78 antibodies. To determine the endocytosed viral load in siRNA-transfected cells (48 h posttransfection), the cells were incubated with JEV at an MOI of 5 on ice for 1 h, followed by one PBS wash and a shift to 37°C for 2 h with complete medium. After incubation, the cells were washed with chilled PBS, followed by proteinase K treatment (1 mg/ml) for 45 min at 4°C, followed by addition of phenylmethylsulfonyl fluoride (PMSF) (2 mM) to quench the proteinase K activity. The cells were then lysed with TRIzol reagent, and endocytosed JEV RNA was quantified by qRT-PCR. The proteinase K treatment ensured that any membrane-bound virions that had not been internalized were removed. The efficacy of the proteinase K treatment to remove surface-bound virus particles was established.

Antibody inhibition assays for JEV infection. To check for inhibition of JEV infection by GRP78/MHC-I antibodies, cells were incubated with 100 μg/ml of the specific rabbit antibodies or rabbit IgG (negative control) for 1 h on ice, followed by two washes with chilled PBS. JEV (MOI, 1) was added to the cells for 30 min on ice, followed by 1 h at 37°C. The cells were then washed twice with PBS, and complete medium was added. After 24 h, the cells were lysed in TRIzol reagent, and JEV RNA levels were determined by qRT-PCR. Virus titers in the supernatant of infected cells were estimated by plaque assays (73).

Immunostaining and fluorescence microscopy. For all immunofluorescence experiments, cells were grown on coverslips (Becton Dickinson) or in 96-well imaging plates (Eppendorf). Purified JEV ED3 or NS3 (1 mg/ml) was labeled with Alexa Fluor 568 dye using an Alexa Fluor 568 protein-labeling kit (Invitrogen). Protein binding of cells was analyzed by adding Alexa Fluor 568-coupled ED3 or NS3 to the cells for 1 h on ice, followed by PBS washing and fixation of the cells with 2% paraformaldehyde. For membrane staining of GRP78, live cells were incubated with GRP78 antibody, followed by Alexa 488-coupled appropriate secondary antibody on ice, followed by fixation. This protocol essentially ensures staining of only plasma membrane proteins and has been independently confirmed by costaining with membrane lipid dyes. For JEV infection experiments and for colocalization studies, cells were fixed in 2% paraformaldehyde at 24 h p.i. and permeabilized with 0.1% Triton X-100–0.4% saponin for 20 min at room temperature, followed by staining with primary and appropriate fluorescence-labeled secondary antibodies. Cells were mounted using ProLong Gold anti-fade reagent with DAPI. Images were acquired on an Olympus FV1000 confocal microscope with 20× (numerical aperture [NA], 1.2) or 60× (NA, 1.4) Plan Apo objectives. Z-stacks were acquired by sequential scanning, and FluoView software was used to generate cross-sectional and maximum-intensity projection images. The colocalization index was calculated using FluoView software.

Immunoprecipitation. Immunoprecipitations were performed with JEV-infected (MOI, 10) Neuro2a/Huh-7 cells plated in 100-mm dishes. At 24 h p.i., the cells were lysed by adding 0.5 ml lysis buffer (20 mM

Tris HCl, 1 mM EDTA, 250 mM NaCl, 1% Triton X-100, 1 mM PMSF, 1 mM protease inhibitor). The total cell lysate was precleared with protein G or protein A beads. This was followed by addition of 5 μg JEV E (ab81193)-mouse IgG or 10 μg GRP78 (ab32618)-rabbit IgG antibodies for 6 to 8 h, followed by immobilization with protein G or protein A beads, respectively. Bound proteins from the beads were eluted using SDS sample buffer and analyzed by gel electrophoresis and Western blotting.

SubAB cleavage of GRP78. Recombinant SubAB and $SubA_{A272}B$ mutant toxins were purified as previously described (74, 75). The biological activity of the toxin was established by the cleavage of the 78-kDa GRP78 in toxin-treated Neuro2a and Huh-7 cells, resulting in the appearance of a 28-kDa C-terminal fragment detectable with the C-terminus-specific GRP78 antibody. JEV-infected cells were either mock treated or treated with SubAB or $SubA_{A272}B$ mutant toxin (50 to 100 ng/ml) at the indicated times p.i. and maintained until 24 h p.i. The cells were then processed for RNA extraction, immunofluorescence, and Western blotting.

JEV RNA isolation and transfection. JEV RNA was isolated from purified JEV virions using the QIAamp viral RNA minikit (catalog no. 52904). Neuro2a cells were seeded in 12-well plates and 24 h later transfected with NT or GRP78 siRNA. After 48 h of siRNA treatment, the cells were transfected with 300 ng JEV RNA using Lipofectamine 2000, and 24 h later, the culture supernatant and cells were processed for plaque assays, qRT-PCR, and Western blotting.

MTT assay. Cells were seeded in 96-well plates. After 24 h, toxin or siRNA treatment was given in triplicate. After 24, 48, or 72 h, MTT (Amresco; 0793-1G) was added to the cells at a final concentration of 0.5 mg/ml. After 3 h of incubation with MTT solution, the entire medium was removed, and the assay was terminated by adding 100 μl dimethyl sulfoxide (DMSO) per well. Readings were taken at 570 nm using an enzyme-linked immunosorbent assay (ELISA) plate reader. The percent cell viability was calculated as follows: [(absorbance for toxin/siRNA-treated cells)/(absorbance for mock-treated cells)] $\times$ 100.

Statistical analysis. Student's *t* test was used for statistical analysis. Differences were considered significant at *P* values of <0.05 and <0.01.

ACKNOWLEDGMENTS

We thank Vishal Gupta for NS3 cloning and purification protocols and Shailendra Chauhan for assistance with virus production and purification. The C-CAMP Mass Spectrometry Facility and Dominik Schwudke are acknowledged for their technical services.

This work was supported by research grant 5203-3 from the Indo-French Centre for the Promotion of Advanced Research (IFCPAR) to M.K. and grant BT/MB/01/VIDRC/08 from the Department of Biotechnology, Ministry of Science and Technology, to S.V. A.B. acknowledges support from a Tata Innovation Fellowship (BT/HRD/35/01/02/2014) and S.M. from a DST Inspire Fellowship (IF/140074). M.N. was supported by a CSIR fellowship.

REFERENCES

1. Daep CA, Munoz-Jordan JL, Eugenin EA. 2014. Flaviviruses, an expanding threat in public health: focus on dengue, West Nile, and Japanese encephalitis virus. J Neurovirol 20:539–560. https://doi.org/10.1007/s13365-014-0285-z.
2. Ghosh D, Basu A. 2009. Japanese encephalitis—a pathological and clinical perspective. PLoS Negl Trop Dis 3:e437. https://doi.org/10.1371/journal.pntd.0000437.
3. Wang H, Liang G. 2015. Epidemiology of Japanese encephalitis: past, present, and future prospects. Ther Clin Risk Manag 11:435–448. https://doi.org/10.2147/TCRM.S51168.
4. Lindenbach BD, Thiel H-J, Rice CM. 2007. Flaviviridae: the viruses and their replication, p 1101–1152. *In* Knipe DM, Howley PM (ed), Fields virology, 5th ed, vol 1. Lippincott-Raven Publishers, Philadelphia, PA.
5. Luca VC, AbiMansour J, Nelson CA, Fremont DH. 2012. Crystal structure of the Japanese encephalitis virus envelope protein. J Virol 86:2337–2346. https://doi.org/10.1128/JVI.06072-11.
6. Crill WD, Roehrig JT. 2001. Monoclonal antibodies that bind to domain III of dengue virus E glycoprotein are the most efficient blockers of virus adsorption to Vero cells. J Virol 75:7769–7773. https://doi.org/10.1128/JVI.75.16.7769-7773.2001.
7. Modis Y, Ogata S, Clements D, Harrison SC. 2003. A ligand-binding pocket in the dengue virus envelope glycoprotein. Proc Natl Acad Sci U S A 100:6986–6991. https://doi.org/10.1073/pnas.0832193100.
8. Rey FA, Heinz FX, Mandl C, Kunz C, Harrison SC. 1995. The envelope glycoprotein from tick-borne encephalitis virus at 2 A resolution. Nature 375:291–298. https://doi.org/10.1038/375291a0.
9. Wu KP, Wu CW, Tsao YP, Kuo TW, Lou YC, Lin CW, Wu SC, Cheng JW. 2003. Structural basis of a flavivirus recognized by its neutralizing antibody: solution structure of the domain III of the Japanese encephalitis virus envelope protein. J Biol Chem 278:46007–46013. https://doi.org/10.1074/jbc.M307776200.
10. Chien YJ, Chen WJ, Hsu WL, Chiou SS. 2008. Bovine lactoferrin inhibits Japanese encephalitis virus by binding to heparan sulfate and receptor for low density lipoprotein. Virology 379:143–151. https://doi.org/10.1016/j.virol.2008.06.017.
11. Chiou SS, Liu H, Chuang CK, Lin CC, Chen WJ. 2005. Fitness of Japanese encephalitis virus to Neuro-2a cells is determined by interactions of the viral envelope protein with highly sulfated glycosaminoglycans on the cell surface. J Med Virol 76:583–592. https://doi.org/10.1002/jmv.20406.
12. Su CM, Liao CL, Lee YL, Lin YL. 2001. Highly sulfated forms of heparin sulfate are involved in Japanese encephalitis virus infection. Virology 286:206–215. https://doi.org/10.1006/viro.2001.0986.
13. Wang P, Hu K, Luo S, Zhang M, Deng X, Li C, Jin W, Hu B, He S, Li M, Du T, Xiao G, Zhang B, Liu Y, Hu Q. 2016. DC-SIGN as an attachment factor mediates Japanese encephalitis virus infection of human dendritic cells via interaction with a single high-mannose residue of viral E glycoprotein. Virology 488:108–119. https://doi.org/10.1016/j.virol.2015.11.006.
14. Chu JJ, Ng ML. 2004. Interaction of West Nile virus with alpha v beta 3 integrin mediates virus entry into cells. J Biol Chem 279:54533–54541. https://doi.org/10.1074/jbc.M410208200.
15. Das S, Laxminarayana SV, Chandra N, Ravi V, Desai A. 2009. Heat shock protein 70 on Neuro2a cells is a putative receptor for Japanese encephalitis virus. Virology 385:47–57. https://doi.org/10.1016/j.virol.2008.10.025.
16. Nain M, Abdin MZ, Kalia M, Vrati S. 2016. Japanese encephalitis virus

invasion of cell: allies and alleys. Rev Med Virol 26:129–141. https://doi.org/10.1002/rmv.1868.
17. Ren J, Ding T, Zhang W, Song J, Ma W. 2007. Does Japanese encephalitis virus share the same cellular receptor with other mosquito-borne flaviviruses on the C6/36 mosquito cells? Virol J 4:83. https://doi.org/10.1186/1743-422X-4-83.
18. Thongtan T, Wikan N, Wintachai P, Rattanarungsan C, Srisomsap C, Cheepsunthorn P, Smith DR. 2012. Characterization of putative Japanese encephalitis virus receptor molecules on microglial cells. J Med Virol 84:615–623. https://doi.org/10.1002/jmv.23248.
19. Gething MJ, Sambrook J. 1992. Protein folding in the cell. Nature 355:33–45. https://doi.org/10.1038/355033a0.
20. Li J, Lee AS. 2006. Stress induction of GRP78/BiP and its role in cancer. Curr Mol Med 6:45–54. https://doi.org/10.2174/156652406775574523.
21. Quinones QJ, de Ridder GG, Pizzo SV. 2008. GRP78: a chaperone with diverse roles beyond the endoplasmic reticulum. Histol Histopathol 23:1409–1416.
22. Bellani S, Mescola A, Ronzitti G, Tsushima H, Tilve S, Canale C, Valtorta F, Chieregatti E. 2014. GRP78 clustering at the cell surface of neurons transduces the action of exogenous alpha-synuclein. Cell Death Differ 21:1971–1983. https://doi.org/10.1038/cdd.2014.111.
23. Bhattacharjee G, Ahamed J, Pedersen B, El-Sheikh A, Mackman N, Ruf W, Liu C, Edgington TS. 2005. Regulation of tissue factor-mediated initiation of the coagulation cascade by cell surface grp78. Arterioscler Thromb Vasc Biol 25:1737–1743. https://doi.org/10.1161/01.ATV.0000173419.31242.56.
24. Honda T, Horie M, Daito T, Ikuta K, Tomonaga K. 2009. Molecular chaperone BiP interacts with Borna disease virus glycoprotein at the cell surface. J Virol 83:12622–12625. https://doi.org/10.1128/JVI.01201-09.
25. Jindadamrongwech S, Thepparit C, Smith DR. 2004. Identification of GRP 78 (BiP) as a liver cell expressed receptor element for dengue virus serotype 2. Arch Virol 149:915–927. https://doi.org/10.1007/s00705-003-0263-x.
26. Philippova M, Ivanov D, Joshi MB, Kyriakakis E, Rupp K, Afonyushkin T, Bochkov V, Erne P, Resink TJ. 2008. Identification of proteins associating with glycosylphosphatidylinositol-anchored T-cadherin on the surface of vascular endothelial cells: role for Grp78/BiP in T-cadherin-dependent cell survival. Mol Cell Biol 28:4004–4017. https://doi.org/10.1128/MCB.00157-08.
27. Triantafilou K, Fradelizi D, Wilson K, Triantafilou M. 2002. GRP78, a coreceptor for coxsackievirus A9, interacts with major histocompatibility complex class I molecules which mediate virus internalization. J Virol 76:633–643. https://doi.org/10.1128/JVI.76.2.633-643.2002.
28. Chevalier M, Rhee H, Elguindi EC, Blond SY. 2000. Interaction of murine BiP/GRP78 with the DnaJ homologue MTJ1. J Biol Chem 275:19620–19627. https://doi.org/10.1074/jbc.M001333200.
29. Earl PL, Moss B, Doms RW. 1991. Folding, interaction with GRP78-BiP, assembly, and transport of the human immunodeficiency virus type 1 envelope protein. J Virol 65:2047–2055.
30. Triantafilou M, Fradelizi D, Triantafilou K. 2001. Major histocompatibility class one molecule associates with glucose regulated protein (GRP) 78 on the cell surface. Hum Immunol 62:764–770. https://doi.org/10.1016/S0198-8859(01)00269-5.
31. Oliphant T, Nybakken GE, Engle M, Xu Q, Nelson CA, Sukupolvi-Petty S, Marri A, Lachmi BE, Olshevsky U, Fremont DH, Pierson TC, Diamond MS. 2006. Antibody recognition and neutralization determinants on domains I and II of West Nile Virus envelope protein. J Virol 80:12149–12159. https://doi.org/10.1128/JVI.01732-06.
32. Chin JF, Chu JJ, Ng ML. 2007. The envelope glycoprotein domain III of dengue virus serotypes 1 and 2 inhibit virus entry. Microbes Infect 9:1–6. https://doi.org/10.1016/j.micinf.2006.09.009.
33. Chu JJ, Rajamanonmani R, Li J, Bhuvanakantham R, Lescar J, Ng ML. 2005. Inhibition of West Nile virus entry by using a recombinant domain III from the envelope glycoprotein. J Gen Virol 86:405–412. https://doi.org/10.1099/vir.0.80411-0.
34. Fan J, Liu Y, Xie X, Zhang B, Yuan Z. 2013. Inhibition of Japanese encephalitis virus infection by flavivirus recombinant E protein domain III. Virol Sin 28:152–160. https://doi.org/10.1007/s12250-013-3331-8.
35. Zu X, Liu Y, Wang S, Jin R, Zhou Z, Liu H, Gong R, Xiao G, Wang W. 2014. Peptide inhibitor of Japanese encephalitis virus infection targeting envelope protein domain III. Antiviral Res 104:7–14. https://doi.org/10.1016/j.antiviral.2014.01.011.
36. Rosenberg E, Taher MM, Kuemmerle NB, Farnsworth J, Valerie K. 2001. A truncated human xeroderma pigmentosum complementation group A protein expressed from an adenovirus sensitizes human tumor cells to ultraviolet light and cisplatin. Cancer Res 61:764–770.
37. Kalia M, Khasa R, Sharma M, Nain M, Vrati S. 2013. Japanese encephalitis virus infects neuronal cells through a clathrin-independent endocytic mechanism. J Virol 87:148–162. https://doi.org/10.1128/JVI.01399-12.
38. Tsai YL, Zhang Y, Tseng CC, Stanciauskas R, Pinaud F, Lee AS. 2015. Characterization and mechanism of stress-induced translocation of 78-kilodalton glucose-regulated protein (GRP78) to the cell surface. J Biol Chem 290:8049–8064. https://doi.org/10.1074/jbc.M114.618736.
39. Wati S, Soo ML, Zilm P, Li P, Paton AW, Burrell CJ, Beard M, Carr JM. 2009. Dengue virus infection induces upregulation of GRP78, which acts to chaperone viral antigen production. J Virol 83:12871–12880. https://doi.org/10.1128/JVI.01419-09.
40. Paton AW, Beddoe T, Thorpe CM, Whisstock JC, Wilce MC, Rossjohn J, Talbot UM, Paton JC. 2006. AB5 subtilase cytotoxin inactivates the endoplasmic reticulum chaperone BiP. Nature 443:548–552. https://doi.org/10.1038/nature05124.
41. Bhullar D, Jalodia R, Kalia M, Vrati S. 2014. Cytoplasmic translocation of polypyrimidine tract-binding protein and its binding to viral RNA during Japanese encephalitis virus infection inhibits virus replication. PLoS One 9:e114931. https://doi.org/10.1371/journal.pone.0114931.
42. Sharma M, Bhattacharyya S, Nain M, Kaur M, Sood V, Gupta V, Khasa R, Abdin MZ, Vrati S, Kalia M. 2014. Japanese encephalitis virus replication is negatively regulated by autophagy and occurs on LC3-I- and EDEM1-containing membranes. Autophagy 10:1637–1651. https://doi.org/10.4161/auto.29455.
43. Gonzalez-Gronow M, Selim MA, Papalas J, Pizzo SV. 2009. GRP78: a multifunctional receptor on the cell surface. Antioxid Redox Signal 11:2299–2306. https://doi.org/10.1089/ars.2009.2568.
44. Ni M, Zhang Y, Lee AS. 2011. Beyond the endoplasmic reticulum: atypical GRP78 in cell viability, signalling and therapeutic targeting. Biochem J 434:181–188. https://doi.org/10.1042/BJ20101569.
45. Misra UK, Gonzalez-Gronow M, Gawdi G, Wang F, Pizzo SV. 2004. A novel receptor function for the heat shock protein Grp78: silencing of Grp78 gene expression attenuates alpha2M*-induced signalling. Cell Signal 16:929–938. https://doi.org/10.1016/j.cellsig.2004.01.003.
46. Gonzalez-Gronow M, Kaczowka SJ, Payne S, Wang F, Gawdi G, Pizzo SV. 2007. Plasminogen structural domains exhibit different functions when associated with cell surface GRP78 or the voltage-dependent anion channel. J Biol Chem 282:32811–32820. https://doi.org/10.1074/jbc.M703342200.
47. Kim KB, Lee JW, Lee CS, Kim BW, Choo HJ, Jung SY, Chi SG, Yoon YS, Yoon G, Ko YG. 2006. Oxidation-reduction respiratory chains and ATP synthase complex are localized in detergent-resistant lipid rafts. Proteomics 6:2444–2453. https://doi.org/10.1002/pmic.200500574.
48. Misra UK, Pizzo SV. 2008. Heterotrimeric Galphaq11 co-immunoprecipitates with surface-anchored GRP78 from plasma membranes of alpha2M*-stimulated macrophages. J Cell Biochem 104:96–104. https://doi.org/10.1002/jcb.21607.
49. Triantafilou K, Triantafilou M. 2003. Lipid raft microdomains: key sites for Coxsackievirus A9 infectious cycle. Virology 317:128–135. https://doi.org/10.1016/j.virol.2003.08.036.
50. Zhu YZ, Cao MM, Wang WB, Wang W, Ren H, Zhao P, Qi ZT. 2012. Association of heat-shock protein 70 with lipid rafts is required for Japanese encephalitis virus infection in Huh7 cells. J Gen Virol 93:61–71. https://doi.org/10.1099/vir.0.034637-0.
51. Hurtley SM, Bole DG, Hoover-Litty H, Helenius A, Copeland CS. 1989. Interactions of misfolded influenza virus hemagglutinin with binding protein (BiP). J Cell Biol 108:2117–2126. https://doi.org/10.1083/jcb.108.6.2117.
52. Ng DT, Randall RE, Lamb RA. 1989. Intracellular maturation and transport of the SV5 type II glycoprotein hemagglutinin-neuraminidase: specific and transient association with GRP78-BiP in the endoplasmic reticulum and extensive internalization from the cell surface. J Cell Biol 109:3273–3289. https://doi.org/10.1083/jcb.109.6.3273.
53. Machamer CE, Doms RW, Bole DG, Helenius A, Rose JK. 1990. Heavy chain binding protein recognizes incompletely disulfide-bonded forms of vesicular stomatitis virus G protein. J Biol Chem 265:6879–6883.
54. Roux L. 1990. Selective and transient association of Sendai virus HN glycoprotein with BiP. Virology 175:161–166. https://doi.org/10.1016/0042-6822(90)90196-X.
55. Mulvey M, Brown DT. 1995. Involvement of the molecular chaperone BiP in maturation of Sindbis virus envelope glycoproteins. J Virol 69:1621–1627.

56. Gaudin Y. 1997. Folding of rabies virus glycoprotein: epitope acquisition and interaction with endoplasmic reticulum chaperones. J Virol 71: 3742–3750.
57. Choukhi A, Ung S, Wychowski C, Dubuisson J. 1998. Involvement of endoplasmic reticulum chaperones in the folding of hepatitis C virus glycoproteins. J Virol 72:3851–3858.
58. Cho DY, Yang GH, Ryu CJ, Hong HJ. 2003. Molecular chaperone GRP78/BiP interacts with the large surface protein of hepatitis B virus in vitro and in vivo. J Virol 77:2784–2788. https://doi.org/10.1128/JVI.77.4.2784-2788.2003.
59. Buchkovich NJ, Maguire TG, Yu Y, Paton AW, Paton JC, Alwine JC. 2008. Human cytomegalovirus specifically controls the levels of the endoplasmic reticulum chaperone BiP/GRP78, which is required for virion assembly. J Virol 82:31–39. https://doi.org/10.1128/JVI.01881-07.
60. Limjindaporn T, Wongwiwat W, Noisakran S, Srisawat C, Netsawang J, Puttikhunt C, Kasinrerk W, Avirutnan P, Thiemmeca S, Sriburi R, Sittisombut N, Malasit P, Yenchitsomanus PT. 2009. Interaction of dengue virus envelope protein with endoplasmic reticulum-resident chaperones facilitates dengue virus production. Biochem Biophys Res Commun 379:196–200. https://doi.org/10.1016/j.bbrc.2008.12.070.
61. Maruri-Avidal L, Lopez S, Arias CF. 2008. Endoplasmic reticulum chaperones are involved in the morphogenesis of rotavirus infectious particles. J Virol 82:5368–5380. https://doi.org/10.1128/JVI.02751-07.
62. Wu YP, Chang CM, Hung CY, Tsai MC, Schuyler SC, Wang RY. 2011. Japanese encephalitis virus co-opts the ER-stress response protein GRP78 for viral infectivity. Virol J 8:128. https://doi.org/10.1186/1743-422X-8-128.
63. Hampton RY. 2000. ER stress response: getting the UPR hand on misfolded proteins. Curr Biol 10:R518–R521. https://doi.org/10.1016/S0960-9822(00)00583-2.
64. Lee AS. 2005. The ER chaperone and signaling regulator GRP78/BiP as a monitor of endoplasmic reticulum stress. Methods 35:373–381. https://doi.org/10.1016/j.ymeth.2004.10.010.
65. Jordan R, Wang L, Graczyk TM, Block TM, Romano PR. 2002. Replication of a cytopathic strain of bovine viral diarrhea virus activates PERK and induces endoplasmic reticulum stress-mediated apoptosis of MDBK cells. J Virol 76:9588–9599. https://doi.org/10.1128/JVI.76.19.9588-9599.2002.
66. Joyce MA, Walters KA, Lamb SE, Yeh MM, Zhu LF, Kneteman N, Doyle JS, Katze MG, Tyrrell DL. 2009. HCV induces oxidative and ER stress, and sensitizes infected cells to apoptosis in SCID/Alb-uPA mice. PLoS Pathog 5:e1000291. https://doi.org/10.1371/journal.ppat.1000291.
67. Su HL, Liao CL, Lin YL. 2002. Japanese encephalitis virus infection initiates endoplasmic reticulum stress and an unfolded protein response. J Virol 76:4162–4171. https://doi.org/10.1128/JVI.76.9.4162-4171.2002.
68. Wolfson JJ, May KL, Thorpe CM, Jandhyala DM, Paton JC, Paton AW. 2008. Subtilase cytotoxin activates PERK, IRE1 and ATF6 endoplasmic reticulum stress-signalling pathways. Cell Microbiol 10:1775–1786. https://doi.org/10.1111/j.1462-5822.2008.01164.x.
69. Yamazaki H, Hiramatsu N, Hayakawa K, Tagawa Y, Okamura M, Ogata R, Huang T, Nakajima S, Yao J, Paton AW, Paton JC, Kitamura M. 2009. Activation of the Akt-NF-kappaB pathway by subtilase cytotoxin through the ATF6 branch of the unfolded protein response. J Immunol 183: 1480–1487. https://doi.org/10.4049/jimmunol.0900017.
70. Sun S, Shi G, Sha H, Ji Y, Han X, Shu X, Ma H, Inoue T, Gao B, Kim H, Bu P, Guber RD, Shen X, Lee AH, Iwawaki T, Paton AW, Paton JC, Fang D, Tsai B, Yates JR, III, Wu H, Kersten S, Long Q, Duhamel GE, Simpson KW, Qi L. 2015. IRE1alpha is an endogenous substrate of endoplasmic-reticulum-associated degradation. Nat Cell Biol 17:1546–1555. https://doi.org/10.1038/ncb3266.
71. Bhattacharyya S, Sen U, Vrati S. 2014. Regulated IRE1-dependent decay pathway is activated during Japanese encephalitis virus-induced unfolded protein response and benefits viral replication. J Gen Virol 95: 71–79. https://doi.org/10.1099/vir.0.057265-0.
72. Ghosh S, Mukherjee S, Basu A. 2015. Chandipura virus perturbs cholesterol homeostasis leading to neuronal apoptosis. J Neurochem 135: 368–380. https://doi.org/10.1111/jnc.13208.
73. Vrati S, Agarwal V, Malik P, Wani SA, Saini M. 1999. Molecular characterization of an Indian isolate of Japanese encephalitis virus that shows an extended lag phase during growth. J Gen Virol 80:1665–1671. https://doi.org/10.1099/0022-1317-80-7-1665.
74. Paton AW, Srimanote P, Talbot UM, Wang H, Paton JC. 2004. A new family of potent AB(5) cytotoxins produced by Shiga toxigenic Escherichia coli. J Exp Med 200:35–46. https://doi.org/10.1084/jem.20040392.
75. Talbot UM, Paton JC, Paton AW. 2005. Protective immunization of mice with an active-site mutant of subtilase cytotoxin of Shiga toxin-producing Escherichia coli. Infect Immun 73:4432–4436. https://doi.org/10.1128/IAI.73.7.4432-4436.2005.